Norges miljø- og
biovitenskapelige
universitet

Master thesis 2023 30 ECTS
Faculty of Environmental Sciences and Natural Resource Management

Estimation of wood dust content in mixed air samples from prepared samples and samples from a construction site by using low thermal plasma decomposition

Niclas Hurtig
Master in Enviromental sciences

Preface

This thesis marks the end of a two-year run for a master's in environmental sciences at the Faculty of Environmental Sciences and Natural Resource Management (MINA), at the University of Life Sciences (NMBU). The thesis has been a part of the BYGGX project at The National Institute of Occupational Health in Norway (STAMI).

I want to thank you my two supervisors Pål Graff (Senior scientist at STAMI) and Torunn K. Ervik (Scientist at STAMI). I would also thank Kari Dahl (Senior engineer) for the help with x-ray diffraction analysis and Johanne Halvorsen (PhD candidate) for the assistance with the field sampling. I am grateful for their support and guidance during these last months. At times it has been frustrating and difficult to understand how to approach and complete the work undertaken. I appreciate the enthusiasm and positiveness you both have shown towards the thesis. Yor inputs and discussions have been of great value, keeping up my motivation to finish this degree.

I would also thank all the nice people at STAMI and especially the Occupational Environmental Chemistry group for including me in your group during lunch and coffee breaks. This has enlightened my day during the months I have been working and struggling with the master thesis.

The last 5 years at NMBU has been an interesting experience. Little did I know after leaving the army after 6 years that I would be in the position I am in today. There have been times where I have doubted myself, struggling through the academic life, not knowing if the path I have chosen were right. 5 years later, I still don't have any good answers. I want to thank all my friends. You are my extended family and I know I couldn't have achieved a degree without your support.

I am looking forward to using my gained experiences in ways I can't comprehend now, hopefully making a lasting contribution.

Niclas Hurtig

Abstract

A low thermal plasma gravimetric method was used to increase accuracy when measuring wood dust in respirable and total dust. Test samples (n= 37) for total dust were prepared by collecting dust with the combinations of only wood (n=12), wood and gypsum (n=9), wood and quartz (n=6) and wood, quartz, and gypsum (n=10) dust onto PVC fibre filters. The average difference between the measured and loaded mass of wood was in the range of 88-236,1 %. Filters with wood and wood and quartz had the lowest difference between loaded and measured wood after decomposition. The largest differences were observed in the combinations wood and gypsum and wood, gypsum and quartz.

Total dust (n=20) and respirable dust (n=20) was collected during two days from one construction site where rehabilitation was undertaken. The low thermal plasma gravimetric method was applied to the samples. The workplace wood dust results averaged at 19 % for total dust. For the respirable dust, the wood dust content averaged at 10%. 10 respirable dust samples were analyzed with x-ray diffraction (XRD) for α-quartz. The α-quartz were present at all the filters and accounted for an average of 4,5 % of the residue mass. In the respirable dust fraction analyzed, the α-quartz was estimated to be between 0,009 – 0,032 mg/m^3. XRD with the Rietveld method was applied to 10 total dust samples as a complimentary approach to explain the composition of the remaining total dust. The median proportion of the mineral dust contained calcite, quartz, and feldspar, these accounted for 92% of the inorganic residue. The proportion of mineral dust on individual filters varied. Correction of mass loss after decomposition, the estimated content in the air was on average for α-quartz 0,1 mg/m^3, for calcite at 0,49 mg/m^3 and feldspar at 0,19 mg/m^3.

The results from the construction site indicated that the application of this method would be a better approach, than only relying on the total and respirable concentrations alone after sampling. Without the method used in this work, the wood dust exposure would have been overestimated. Furthermore, it indicated that wood dust is not the biggest contributor to particulate matter at construction sites where rehabilitation is being undertaken and that inorganic residue is the largest contributor for exposure to workers.

Sammendrag

En lav temperatur plasma gravimetrisk metode ble brukt for bedre bestemme trestøv i respirabelt og totalt støv prøver. Testprøver (n=37) for totalt støv ble tillaget ved å samle støv med kombinasjonene av kun tre (n=12), tre og gips (n=9), tre og kvarts (n=6) og tre, kvarts og gips (n=10) støv på PVC-fiberfiltre. Den gjennomsnittlige forskjellen mellom målt og belastet mengde med trestøv var 88-236,1 %. Filtre med tre og tre og kvarts hadde de laveste forskjellene mellom belastet og målt tre støv etter dekomponering. De største forskjellene ble observert i kombinasjonene med tre og gips og tre, gips og kvarts.

Prøver for totalt støv (n=20) og respirabelt støv (n=20) ble innsamlet i løpet av to dager fra en byggeplass der rehabilitering ble utført. Lav temperatur plasma gravimetriske metoden ble benyttet på prøvene. For totalt støv ble trestøvfraksjonen estimert til å utgjøre i gjennomsnitt 19 % av det innsamlede partikulære materialet. For det respirable støvet var innholdet av trestøv i gjennomsnitt 10 %. 10 respirable støvprøver ble analysert med røntgendiffraksjon (XRD) for α-kvarts, α-kvartsen var til stede på alle filtrene og utgjorde i gjennomsnitt 4,5 % av den uorganiske massen. I den analyserte respirable støvfraksjonen ble α-kvartsen beregnet til å være mellom 0,009 – 0,032 mg/m^3. XRD med Rietveld-metoden ble brukt på 10 totale støvprøver som en komplementær tilnærming for å forklare sammensetningen av den uorganiske fraksjonen. Medianandelen av mineralstøvet inneholdt kalsitt, kvarts og feltspat, disse utgjorde 92 % av den uorganiske resten. Andelen mineralstøv på individuelle filtrene varierte. Korreksjon av massetap etter dekomponering, ble α-kvarts beregnet til være 0,1 mg/m^3, kalsitt 0,49 mg/m^3 og feltspat 0,19 mg/m^3.

Resultatene fra byggeplassen indikerte at bruk av denne metoden var en bedre tilnærming, enn kun gravimetrisk bestemmelse av total og respirable konsentrasjonene etter prøvetaking. Uten metoden benyttet i dette arbeidet ville trestøveksponeringen blitt overvurdert. Videre indikerte det at trestøv ikke er den største bidragsyteren til PM på byggeplasser der rehabilitering pågår, og at uorganiske rester er den største bidragsyteren til eksponering for arbeidere.

Abbreviations

AM - arithmetic mean

COPD - chronic obstructive pulmonary disease

d_{ae} - aerodynamic diameter

IARC - International Agency for Research on Cancer

LTP - Low temperature plasma

GM - geometric mean

OEL - occupational exposure limits

PM - Particulate matter

PVC - Polyvinylklorid

RCS - respirable crystalline silica

SEM - Scanning electron microscope

SRM - standard reference material

STAMI - The National Institute of Occupational Health in Norway (Norwegian: Statens arbeidsmiljøinstitutt)

STD - standard deviation

TWA - Time weighted average

XRD - X-ray diffraction

WHO - World Health Organization

Table of content

1.0 Introduction

Particulate matter (PM) consists of a heterogenous mixture of solids and liquid droplets. This includes dust, dirt, soot, or smoke. PM can be emitted from several sources related to different types of work, making PM a common occupational hazard. Exposure may vary due to both to the occupations and to the operations undertaken (NOA,2021). According to NOA, 23% of the Norwegian labour force reported they were exposed to polluted air during the workday. A highly exposed group in Norway are employees within the construction industry. More than 58% of the workers in this industry reported they were exposed in some way to PM during the day (NOA, 2021).

Construction work involves the use of a range of materials, the most common being wood, gypsum and concrete. Handling of these generates and emits PM in the working environment, workers are thus exposed to a complex matrix during working hours. Inhalation of PM is dangerous and may have severe health impacts as chronic obstructive pulmonary disease (COPD), asthma and lung cancer (Cheriyan & Choi, 2020). To protect workers against illnesses, occupational exposure limits (OELs) regulate allowed concentration PM in work air, assuring safe work environments for the employees. OEL is an important guidance in trying to keep exposure levels below hazardous values.

As an effort to cut CO_2 emissions, an increased attention towards rehabilitation of older buildings has been seen as a vital solution for the construction sector. Working with rehabilitation will often involve crushing, cutting, sawing, drilling, grinding, and milling inside, making it harder to keep the PM below OEL`s. This is a new challenge, since few air measurements has been sampled under similar conditions with established methods. The current methods are based on pumping air thru filters, and collect PM. After collection, filters are weighed, and the amount of PM is calculated. A problem with this approach, it's that it's not possible to determine the different composition of the sampled PM. If its desirable to know the amount of wood dust it is just assumed that the whole collected weight comes from wood dust. OELs are different for gypsum, wood, and quartz and this nonspecific measurement may overestimate wood dust exposure since it does not consider the presence of mineral dust (Stacey et al., 2019).

In Norway data for wood dust exposures are limited and evidence is needed to assess whether improvements to control measures are required. Better characterization of what type of dust and amount could be an important step to adequately protect workers.

In this thesis, the aim is to further explore methods to better estimate the wood dust collected from air sampling both from prepared samples and from construction sites. The thesis is a cooperation between The National Institute of Occupational Health in Norway (STAMI) and Veidekke as part of the BYGG X project. The work builds upon earlier work undertaken by Stacey (2019. In contrast to Stacey (2019) who used thermal decomposition at 510°C to estimate the wood proportion of collected dust, decomposition of organic material in this thesis was performed by using a low thermal plasma decomposer at 120°C with a continuous flow of O_2. To further investigate the inorganic residue after decomposition, a selection of the sampled material were analyzed by X-ray diffraction in combination with the Rietveld method and SEM – EDS.

With applying these steps, it should be easier to estimate the correct amount of wood dust and inorganic components collected in air samples. Being able to give more accurate information and keep workers safe, therefore the hypothesis of this work was:

- *Low thermal plasma based gravimetric approach increases accuracy when measuring wood dust in complex air samples.*

2.0 Background

According to SSB more than 177 000 are involved or employed directly in the Norwegian construction business (*SSB*, 2022). Construction includes several professions and different tasks for each profession. The transient nature of construction sites makes it difficult to accurately characterize exposures among construction workers (Kirkeskov et al., 2016). This highly changing work environment exposes workers to different levels and types of PM during the day. With a large workforce, many employees have occupational health issues related to their in jobs in construction (Cheriyan & Choi, 2020).

Health impacts depend on the type of inhaled dust and the place in the respiratory tract where it deposits, which is conditioned by the size of its particles (Baran & Teul, 2007). Large particles (more than 100 µm aerodynamic diameter) are unlikely to be inhaled into the nose or mouth, and if they are then they are likely to deposit in the nose or mouth. Smaller particles (below 30 µm) are more likely to be inhaled and deposit in the upper airways. Below 5 – 10 µm aerodynamic diameter, inhaled particles have a reasonable chance of penetrating and depositing in the gas exchange region of the lung. Clearly, insoluble particles that deposit in a specific region of the respiratory track are more likely to produce adverse effects locally at the site of deposition than elsewhere in the body and so the size distribution for this type of aerosol is a key factor in determining health risk (Jiménez et al., n.d)

Numerous scientific studies have linked construction dust exposure to a variety of illnesses (Wang et al., 2023). Wood dust from hard wood processing (beech and oak) has been classified by the International Agency for Research on Cancer (IARC) as a carcinogenic factor (Cancer, 1987). Studies show that occupational exposition to wood dust is strongly connected with the induction of nasal cavity cancer and paranasal sinus cancer (Baran & Teul, 2007)

Silica or quartz is found in many of the most common raw materials used in construction and is a major constituent of construction materials such as bricks, tiles, concrete, and mortar. PM is generated from these materials during many common construction tasks. Some of this dust is fine enough to get deep into your lungs. The fine dust is known as respirable crystalline silica (RCS) and is too fine to see with normal lighting. Inhalation of RCS dust leads to silicosis, a fibrotic lung disease (Baron et al., 2002).

To better safeguard workers against different health impacts, OELs are used as an important regulatory tool (Schenk et al., 2008). OELs are given as time weighted average (TWA). TWA is the employee's average airborne exposure in any 8-hour work shift of a 40-hour work week, which shall not be exceeded. In Norway the OELs for wood, respirable silica and irritating dust are (Arbeidstilsynet, 2021a):

- Wood dust ("soft" Nordic wood types)- 2 mg/m^3 (total dust)
- Wood dust (hard exotic wood types) – 1 mg/m^3 (total dust)
- Irritating dust - 10 mg/m^3 (total dust), respirable (5mg/m^3)
- Quartz - 0.3 mg/m^3 (total dust), 0.05 mg/m^3 (respirable dust)

These amounts are the highest legal amounts that can be accepted in the working air during a day. As mentioned earlier estimation of values in working environments are based on gravimetric measurement dust and these are standardised methods (INRS, 2000). Gravimetrical have disadvantage since their measurements are non-specific, and other airborne components may contribute to the sampled mass.

3.0 Theory

3.1 Particles size

For a perfect spherical particle, the definition is easy, requiring specification only of a single dimension, the particle *geometric diameter* (d). Aerosol in the real word is not spherical, and it is therefore necessary to use metrics as aerodynamic diameter (d_{ae}) that are relevant to describe particles of interest (Vincent, 2007). Aerodynamic diameter is a measure of PM based on size and how particle moves through air, determined by a particles shape and density, permits comparison of particles having irregular shapes and different sizes and densities (Frumkin, 2016).

The World Health Organization (WHO) defines dust as "solid particles, ranging in size from 1 um to 100 um, that may be or become dispersed in the air, depending on their origin, physical characteristics and environmental conditions" (Johnston, 2000).

3.2 Size fractions, inhalable, thoracal, respirable

Exposure to particles is through inhalation with either nose or mouth. The human respiratory are divided into three primary regions as illustrated in Figure 1: the extra thoracic region, tracheobronchial region and the alveolar region. The penetration of particles into the respiratory tract, and hence aerosol exposure of these regions by particle deposition, has seen to be a strong function of particle size (Vincent, 2007).

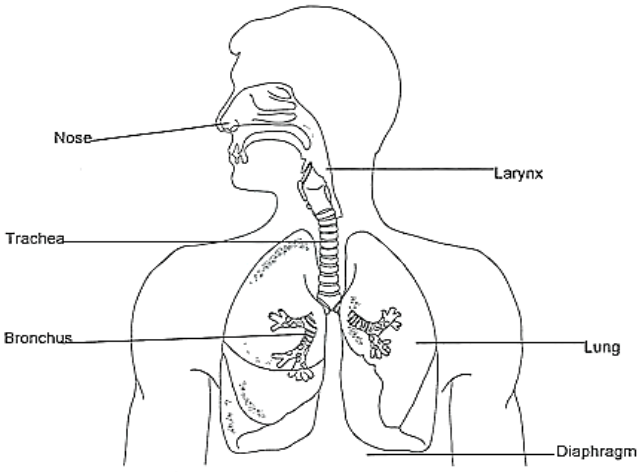

Figure 1: illustration of the human respiratory system (Khan, 2017).

The particles entering the human respiratory system are divided into three different fractions depending on the region the particles may penetrate (Brown et al., 2013; CEN, 1993):

- Inhalable fraction – the mass fraction of total airborne particles which is inhaled through the nose, $d_{ae} \leq 100$ µm.
- Thoracic fraction – the mass fraction of inhaled particles penetrating beyond the larynx, particles with $d_{ae} < 30$ µm and 50% cut – off at 10 µm.
- Respirable fraction – the mass fraction of inhaled particles penetrating to the unciliated airways, particles with $d_{ae} < 10$ µm and 50 % cut-off at 4 µm.

The above definitions are stated in terms of a mass fraction. Relative to total airborne particles, the particle size having 50% penetration for respirable fractions is 4.0 µm d_{ae} and almost 100% penetration at 1 µm d_{ae}, respectively (Brown et al., 2013; CEN, 1993; Hygienists, 2004). Particles with a greater particle size tend to deposit in the head airways. Larger particles, >100 µm, causes irritation in the nose, mouth, and eyes, but will not enter the rest of the respiratory system (Brown et al., 2013).

The different fractions are described in Figure 2. The fractions are given as S-curves, and therefore there is not a linear relationship between the aerodynamic diameter of the airborne particle and its percentage in the fraction. Furthermore, there is not a sharp distinction between the various fractions, which is why a 50% cut-off is defined. That the fractions have a 50% cut-off means that 50% of the total number of airborne particles at the given aerodynamic diameter is deposited in the part of the respiratory system defined by the fraction. For example, with the respirable fraction, 50% of the particles at 4 µm go all the

way down into the bronchioles and alveoli (Brown et al., 2013). The figure also clearly shows where the 50% cut-off for each faction is. This is made visible by the dotted line.

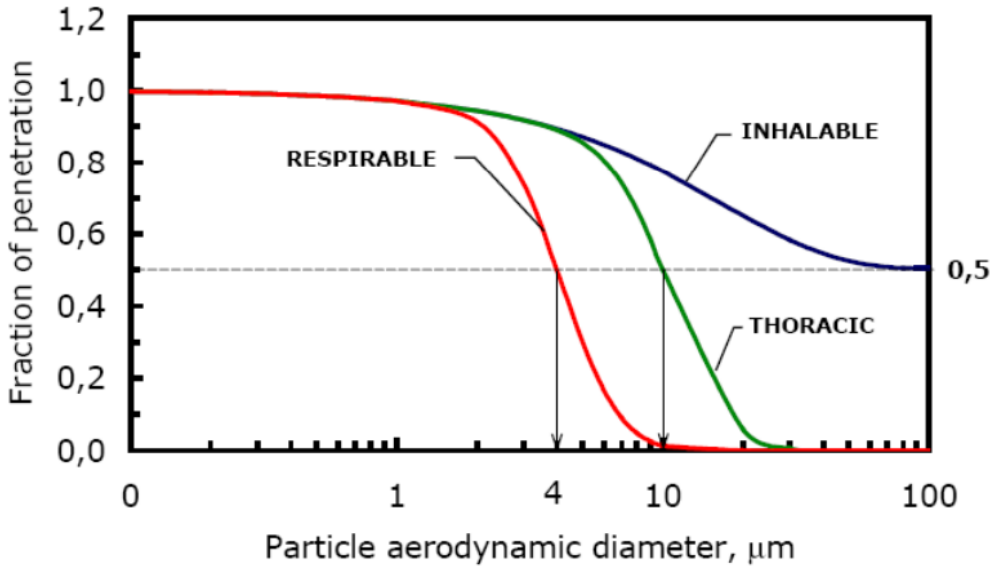

Figure 2:probability of aerosol penetration as a function of aerodynamic diameter, internationally agreed by CEN/IS/ACGHI (Jiménez et al., n.d.)

It is widely understood that the concern of health effects from exposure to particles is not just a function of dose or chemical composition but includes the size of the particle as well (Tatum et al., 2001). A non-health-based fraction who is often been measured historically is the fraction called total dust and it refers to the amount of all airborne PM in a given environment or atmosphere, regardless of size or composition. In earlier years of sampling measuring the total aerosol concentration was seen as a valid approach to determine exposure for workers (Vincent, 2007).

During the 1970`s, occupation hygiene scientist began questioning this the total airborne particulate as a valid health related metric of aerosol exposure(Vincent, 2007). However, this traditional method has created a depth of standardized sampling protocol results for researchers to work with in performing research. “Total dust” can be seen as not providing optimal information regarding the relative size of the particle sampled. Therefore, while total dust measurements can provide important information about overall air quality, they may not be sufficient for assessing specific health risks associated with PM exposure.

3.3 Materials

3.31 Wood

Wood is a material of uneven structure, whose crucial mechanical feature is its toughness, i.e., resistance to deformation caused by the forces acting on its surface. Wood classification by the cell structure divides wood into hardwoods (mostly deciduous trees), and softwoods (mostly conifers). This distinction is purely botanical, softwoods corresponding to the gymnosperms and hardwoods to the angiosperms, and certain characteristics such as the density and hardness of the two types are largely superimposed (Fengel et al., 1989). Wood consists essentially of cellulose, hemicellulose, and lignin.

Several studies have shown that most of wood dust's mass consists of particles with aerodynamic diameters equal or greater than 10 μm (Chung et al., 2000, IARC., 1995, Pisaniello et al., 1991, Whitehead et al., 1981 b). The size of the particles constituting the wood dust depends on the type of operation carried out on the wood; sawing produces particles with larger size than sanding.

On the other hand, the particle size does not seem to depend systematically on the type of wood. For a given process, several studies report very similar particle size distributions between pine and oak; others report that dust from hardwood is finer than dust from softwood (IARC, 1995). Depending on the treatments to which the wood has been subjected before machining, the dust can contain additives, preservatives or adhesives(SCOEL, 2003).

3.32 Quartz

Quartz is a widely distributed mineral of many varieties that consist primarily of silica or silicone dioxide (SiO_2). Quartz is the second most abundant mineral in Earth's crust after feldspar (Humans, 2012). The overwhelming majority of natural crystalline silica exists as α-quartz, who is the thermodynamically stable form of crystalline silica in ambient conditions. Quartz content of ordinary building materials such as concrete, mortar and bricks can be 10-50% (Brendstrup et al., 1990). The silica content in the airborne dusts, however, strongly depends on the amount of silica used in the respective product.

Crystalline silica is probably one of the most documented workplace contaminants; the severity of its health effects and the widespread nature of exposure have been long recognized (Humans, 2012). Overexposure to crystalline silica-containing dust may results in Silicosis who is a fibrotic occupational pulmonary disease (Shtraichman et al., 2015)

RCS refers to the portion of airborne crystalline silica dust that is capable of entering the gas-exchange regions of the lungs if inhaled (*NIOSH Hazard Review*, 2002). Any process that generates RCS, knowing the dust generation rate, the dust size distribution, and the silica content in the dust of different sizes would guide the development of effective and economical engineering control solutions. Field testing of size has proven to be difficult because of varying conditions (Shepherd et al., 2008; Sirianni et al., 2008). A laboratory testing system developed to systematically characterize dust generation rate and size-dependent silica content found that most of the RCS resides in the dust ~2.5 µm in aerodynamic diameter (Qi et al., 2016)

3.33 Gypsum

Gypsum is a white or nearly white, odourless, crystalline solid with chemical formula of $CaSO_4 * 2H_2O$. Calcium sulphate, commonly known as natural gypsum, is found in nature in different forms, mainly as the dihydrate ($CaSO_4 \cdot 2H_2O$) and anhydrite ($CaSO_4$). They are products of partial or total evaporation of inland seas and lakes (Karni & Karni, 1995). It's a common product used in construction. The oral exposure route for gypsum is not a concern because of low oral toxicity. On dissolution in the body, this compound separates into calcium and sulphate ions (Yost et al., 2010)

4.0 Analytical methods

4.1 Low temperature plasma surface decomposition

Low temperature plasmas (LTP), ionized gas (or sometimes liquid), represent a unique state of matter composed of neutral atoms and molecules, radicals, excited states, ions and electrons.(Adamovich et al., 2017)

Applications of plasma are based on arc, microwave and inductively coupled plasma discharges that operate close to thermal equilibrium. When continuously applying energy to a matter, its temperature rises and undergoes the process from solid-state to liquid and gas. Carrying on applying energy, the existing shell of the atom will break up and electrically charged and excited particles and molecule fragments are formed (negatively charged electrons and positively charged ions, radicals). The mixture is called plasma or the fourth state of matter.

In short: changes of the aggregate state under applied energy:

Solid → liquid → gas → plasma

The majority of LTP significantly deviate from thermodynamic equilibrium, with the electron temperature T_e being much higher than the heavy particle temperature and gas temperature T_g. LTP sources can produce a chemically rich environment at close to room temperature both at reduced and at ambient pressures, a unique condition that enables the delivery of highly reactive plasma species (Vardelle et al., 2016)

LTP enables decomposition of materials at low temperatures (~ 120 °C). Oxygen gas is excited in a vacuum by supplying energy, resulting in energetic ions and electrons which constitute the plasma. The oxygen plasma reacts with the organic matter and enables combustion of organic material leaving only the inorganic material from the samples. This reduces the risk of altering any structure characterizing (3-D structures) or chemical composition of the inorganic material.

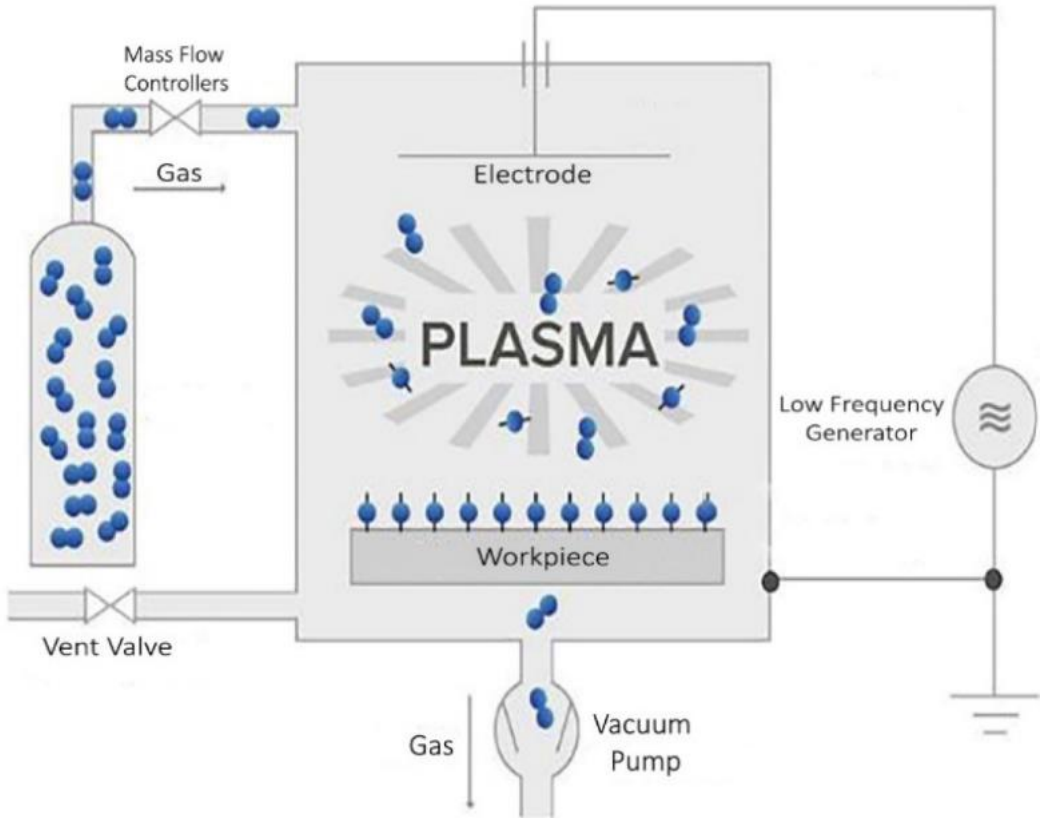

Figure 3: The low-pressure plasma system pumps the gas out of the vacuum chamber and replacing the gas with a process gas at a controlled pressure. This gas is then excited to a plasma state as fresh feed gas is introduced as the vacuum pump continuously removes gas from the process chamber to maintain the process procedure (Sevilla et al., 2020).

4.2 Scanning electron microscope

In Scanning electron microscope, high – energy monochromatic electrons, generated at a potential of 1-30 kV, are formed into finely focused beam which is rastered across the surface of the sample. Electrons are focused by a condenser lens, the high angle electrons are excluded

by an aperture, the beam is then further focused by second condenser lens. Coils sweeps the beam across the surface of the sample in a grid, and an objective lens finally focuses the beam on the sample (Moore & Smart, 2021).

The electrons impinge upon the atoms within an interaction volume close to the surface. This occurs under vacuum conditions, which prevents, and molecules or atoms already present in the microscope column from interacting with the electron beam. This ensures a high quality of imaging. The vacuum also protects the electron source from vibrations and noise. The interaction creates signals produced from the atoms. These include back – scattered electrons, emitted secondary electrons from inelastic scattering and characteristic X-rays. Detectors in the microscope pick up these signals and create high-resolution images displayed on a computer screen (*Britannica, n.d*).

Compared to a light microscope with a useful of 1000x magnification, SEM typically have 200000x magnification and usually achieves a resolution from 0.5 to <20nm depending on the instrument (Hafner, 2007).

4.3 X-ray diffraction

X-ray diffraction is based on constructive interference of monochromatic X-rays and a crystalline sample. It is one of the most important non-destructive instruments used to analyse all kinds of matter ranging from fluids to powders and crystals. The energetic x-rays can penetrate deep into the materials and provide information about the bulk structure (Nasrollahzadeh et al., 2019).

X-rays are electromagnetic radiation with typical photon energies in the range of 100 eV - 100 keV. For diffraction applications, only short wavelength x-rays (hard x-rays) in the range of a few angstroms to 0.1 angstrom (1 keV - 120 keV) are used. These X-rays are generated by a cathode ray tube, filtered to produce monochromatic radiation, collimated to concentrate, and directed toward the sample. As electrons collide with atoms in the target and slow down, a continuous spectrum of x-rays is emitted, which are termed Bremsstrahlung radiation. The high energy electrons also eject inner shell electrons in atoms through the ionization process (Moore & Smart, 2021).

The interaction of the incident rays with the sample produces constructive interference and a diffracted ray when conditions satisfy Braggs law ($n\lambda=2d\sin\theta$). This law relates the wavelength of electromagnetic radiation to the diffraction angle and the lattice spacing in a crystalline sample. These diffracted X-rays are then detected, processed and counted. The

geometry of an X-ray diffractometer is such that the sample rotates in the path of the collimated X-ray beam at an angle θ while the X-ray detector is mounted on an arm to collect the diffracted X-rays and rotates at an angle of 2θ. The instrument used to maintain the angle and rotate the sample is termed a *goniometer*. For typical powder patterns, data is collected at 2θ from ~5° to 70°, angles that are present in the X-ray scan. By scanning the sample through a range of 2θangles, all possible diffraction directions of the lattice should be attained due to the random orientation of the powdered material (*X-Ray Powder Diffraction,* n.d).

Conversion of the diffraction peaks to d-spacings allows identification of the mineral because each mineral has a set of unique d-spacings. Typically, this is achieved by comparison of d-spacings with standard reference patterns.

4.4 Rietveld method

The Rietveld method is a computational process used in conjunction with XRD to provide a multicomponent analysis without the need for calibration of each crystalline component within the sample (Stacey et al., 2019)

This method is based on the Bragg's Law of X-ray diffraction which states that when X-rays are incident on a crystalline material, the X-rays will be scattered in a certain pattern that can be used to determine the structure of the material. The method takes this idea and develops an algorithm to calculate the parameters of the unit cell from the diffraction pattern.

The Rietveld method measures the intensity of X-ray diffraction peaks that are arranged in an interference pattern and is known as the profile. The profile is a graph of the relative intensity of the diffraction peaks as a function of the angle of the incident X-rays. This profile is compared to a simulated profile that is generated by the Rietveld method. The method then adjusts the parameters of the unit cell until a good match is found between the measured and simulated profile (Runčevski & Brown, 2021).

5.0 Methods and materials

5.1 Generation of particulate matter at STAMI

To recreate and produce different fractions of PM under controllable circumstances it was decided to "replicate" similar conditions to those found at a construction site. To accomplish this, a tent was used to have a controlled area where production of PM could be achieved and collected in similar manners as done in field sampling.

A party tent with total size of 3 x 6 meters with a height of 2,3 meters was chosen. Inside the tent, an area of approximately 2,5 x 2,5 meters in size was used to setup up the equipment need to produce and collect PM (se Figure 4). Two types of material were chosen to, wood and gypsum. A handheld grinder with two types of sanding paper, 60 and 80 grit was used to "work" the materials to produce PM. The materials, wood and gypsum were sanded between 1-5 minutes. Sampling was done over two days, first day to produce wood dust and a second day to produce gypsum dust. Between sampling, the filters were weighed to know the amount of wood and gypsum collected at the filters. In addition, after sampling, 10 of the filters was added with quartz in the laboratory. This was to get the combination of gypsum, wood and quartz dust, and wood and quartz dust onto the filters.

Ten Apex2 pro (Casella Solutions., Kempston, UK) pumps were used to simultaneously inside the tent, these pumped air through the filters to collect total dust onto Millipore 25mm 5.0 µm pore-size PVC membrane filters (Millipore Corp., Billerica, MA, USA) placed in closed face "total" aerosol plastic cassettes (Millipore Corp., Billerica, MA, USA). The pumps were calibrated to an airflow of 2.0L/min prior to sampling with a rotameter (Aalborg Instruments & Controls, Inc, New York, USA). The airflow was measured again with the same rotameter after sampling and potential flow changes were corrected for in-data processing.

A real time spectrometer was also used to measure airborne particle concentrations inside the tent. The number of airborne particles from 0.5 to 20 µm d_{ae} was measured by a TSI Incorporated 3321 Aerodynamic Particle Sizer (APS) (Shoreview MN, USA).

Figure 4: The pictures shows the set up inside the "workroom" where PM was produced with the pumps, real time collector, grinder and in this case the wooden material used to produce PM from wood.

5.2 Bulk materials

Samples of wood and gypsum were taken from residue materials at STAMI. No prior analysis was made of the materials before grinding and sanding. The wood material consisted of soft wood types of Nordic origin, most likely Norwegian spruce. Panels of gypsum were used; it was assumed that bulk of the gypsum panels consisted of $CaSO_4$. Quartz (SRM 1878b) was obtained from nist.gov/srm.

5.3 Construction site samples

Samples of PM was collected from one construction site, a rehabilitation project of an old school in central part of Oslo built in 1899. The school is erected in bricks with a plaster coating on the outside and inside of the building, the roof consists of a wooden structure and the isolation consist of a clay material. Sampling was done over two days in mid-February during work hours, flow was measured with a rotameter each day. The building consisted of 4 floors and a basement. The school was sealed off from the outdoors surroundings to protect local environment from noise and air pollution. The main work operations conducted on site were demolition of brick walls, cutting of wood, instalment of walls and floors and bricklaying. Equipment such as table saw, drills and electrical power tools was used. There was no visible ventilation in the building. Heaters were located inside, and they circulated indoor air to produce warmth. Work was conducted between 0700 to 1530. Samples for both total dust and respirable dust were put in pairs inside backpacks and placed at different locations inside the building. No backpacks were carried by workers due to narrow working conditions. Figure 5 gives examples of how the backpacks were place inside the building.

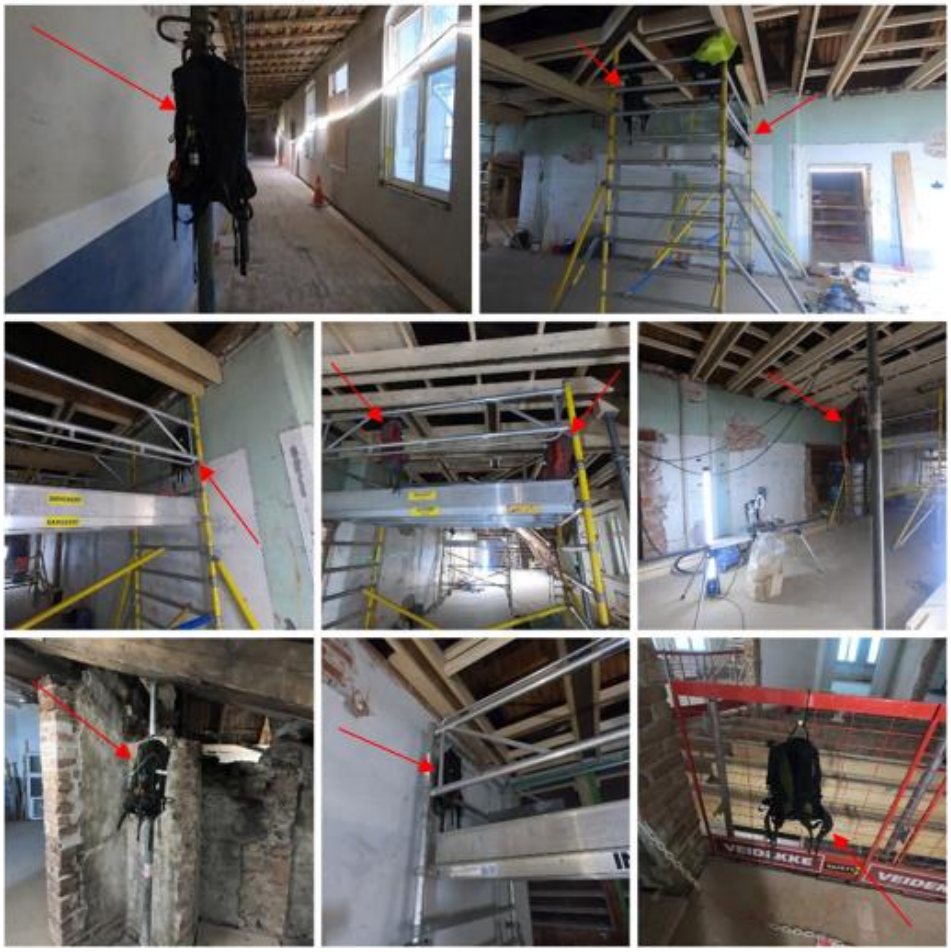

Figure 5: Overview of how the backpacks were placed inside the construction site, red arrows indicate the location of the backpacks with samplers attached.

5.3.1 Collection of total dust and respirable dust at construction sites

Collection of respirable dust and total dust particles were sampled from the site. The pumps were place in pairs inside a backpack. A total of 10 backpacks with 10 pairs of respirable and total dust samplers were placed inside the building. The backpacks were mounted to scaffolds, banisters and posts at different heights and floors. The respirable PM was collected with Higgins-Dewell (JS Holdings, UK) cyclones onto 37 mm 5.0 µm pore-sized polyvinyl chloride filters (PVC) (Millipore Corp., Billerica, MA, USA). A GSA SG5200 pump (Ratingen, Germany) was used to pump air through the filters. The pumps were calibrated to an airflow of 2.2 L/min prior to and after sampling with the same rotameter (Aalborg Instruments & Controls, Inc, New York, USA).

Total dust was collected onto Millipore 25mm 5.0 µm pore-size PVC membrane filters (Millipore Corp., Billerica, MA, USA) placed in closed face "total" aerosol plastic cassettes (Millipore Corp., Billerica, MA, USA). The cassettes were connected to Apex2 pro, and the

pumps were calibrated to an airflow of 2.0L/min prior to sampling with a rotameter (Aalborg Instruments & Controls, Inc, New York, USA). The airflow was measured again with the same rotameter after sampling and potential flow changes were corrected for in-data processing.

5.3.2 Real-time particle number and size measurements at construction site

A real time spectrometer was used to measure airborne particle concentrations at the construction site, a spectrometer was placed in the attic, the 4th. floor, measured continuously during the two days of sampling. The number of airborne particles from 0.5 to 20 µm d_{ae} was measured by a TSI Incorporated 3321 Aerodynamic Particle Sizer (APS) (Shoreview MN, USA).

5.4 Analysis

5.4.1 Gravimetric analysis

All the PVC filters were conditioned in a controlled environment with relative humidity of 40% ± 2% and temperature of 20°C ± 1°C for at least 24 hours before weighing. The filters were then weighed on a Sartorius semi-micro model MC5 balance (Sartorius AG, Göttingen, Germany) before sampling. All samples were conditioned in the same weighing room after sampling and decomposition for at least 48 hours, before being weighed using the same balance. The balance was checked by weighing different weights and a reference filter with known masses prior to the gravimetrical analysis. Unexposed filters (blind filters) were used for correction and weighted at the same time as the samples. All filters were discharged by a radioactive source to minimize static electricity. The filters were weighted to achieve three consistent values within 0.01 mg.

5.4.2 Low temperature plasma decomposition

The filters, both prepared and sampled were treated in a low-temperature plasma decomposition apparatus (Diener electronic GmbH & Co. KG, Ebhausen, Germany) to remove filter substrate and organic material. Samples were decomposed for 120 minutes with a continuous airflow of 25% O_2. After decomposition the residue were suspended in ethanol using an ultrasonic wave-generator and filtrated onto a 25 mm in diameter and 0.45 µm silver membrane filter (Merck Millipore Ltd. Tullagreen, Cork, Ireland). The extraction was done by using a water aspirator connected to a faucet and a water-suction filtration system.

5.4.3 X – ray diffraction

The mass of α-quartz on each of the collected filters was determined by X-ray diffraction spectrometry, using a Malvern Panalytical X'Pert*3*Powder diffractometer, equipped with an Empyrean X-ray tube and a PIXcel*1D* detector (Malvern Panalytical B.V., Eindhoven, Netherlands). 35 collected filters were examined after decomposition and filtration onto silver membrane filters. 12 total and 13 respirable dust samples from construction site, 6 filters loaded with wood, gypsum and quartz, 6 filters loaded with wood and quartz and 3 method blank filters from STAMI.

NIST SRM 2950a was used for calibration and analysis was performed according to the silver filter method (NIOSH Method 7500) for the respirable dust sampled at the construction site. A LOD (3 SD of blank filters) of 2 µg per filter was achieved.

5.4.4 Scanning electron microscope analysis

Particles deposited on the silver membranes were investigated with a Hitachi SU6600 field emission SEM (Hitachi, Tokyo, Japan), equipped with a Bruker energy dispersive X-ray (EDX) detector (Bruker Nano GmbH, Berlin, Germany). Particles were imaged with secondary electrons, while EDS detector was used for element detection. The mapping tool HyperMap was used to map the distribution of elements over an image field.

5.4.5 Data Processing

For data processing two processing program was used for the treatment of data and graphical presentations, Microsoft Office Excel 2016 (Microsoft Corporation, Redmond, WA, USA) and SigmaPlot 14.0 (Systat Software Inc., Palo Alto, CA, USA)

6.0 Results

The results are divided into two parts, the first part shows the results and analysis related to the experiment and work performed at STAMI. The second part shows the data collected at the renovation project from the old school in Oslo. Here the results for sampling and analysis are shown in detail.

6.1 Results from experiments conducted at STAMI

PM was sampled at STAMI as described in the methods and materials. After sampling the filters were weighed to determine collected amount of the different types of material. The collected PM of wood had the lowest average mass with 0,575mg and lowest loading range from 0,141-0,983 mg. The combination of wood, gypsum had the largest average total loading mass with 10,91 mg and the highest loading range from 6,98– 17,64 mg.

Table 1: Averages of the different masses loaded onto filters and the loading range for the laboratory prepared samples.

Matrix of dust on filters	Number of samples	Average mass loading wood dust (mg)	Average mass loading quartz (mg)	Average mass loading gypsum (mg)	Average total loading mass(mg)	Loading range (mg)
Wood	12	0,575	0	0	0,575	0,14-0,98
Wood and Quartz	6	0,767	2,04	0	2,81	2,27-3,67
Wood and Gypsum	9	0,838	0	6,51	7,35	0,56-12,89
Wood, Gypsum and Quartz	10	0,833	2,66	7,41	10,91	6,98-17,64
Total	37					

6.2 Comparison of gravimetric mass of wood, before and after decomposition

The filters were loaded with different amounts of wood, gypsum and quartz as listed in Table 1. After decomposition, the differences were highest when the loaded mass values of wood were relatively low and loaded masses of gypsum was high. For the blank filters of total dust after decomposition the average weight was 0,005 mg and for the respirable dust filters was 0,0035 mg. Comparison between added mass before and after decomposition was done taking the gravimetrically determined residue after extraction and subtracting with the original weight of added wood dust to estimate the removed mass.

6.2.1 Only wood

12 filters were only loaded with wood dust and average added mass was 0,575mg. After decomposition, an average of 0,510 mg had been removed, accounting for 88,5 % removal overall for added wood dust on the filters.

The range of removal was between 60,1 – 98,4 %, for the 12 filters. Figure 6 shows the relationship between before and after decomposition. A simple linear regression was performed, the fitted line had the equation 0,065 + 1,002x and the r^2 was 0,898.

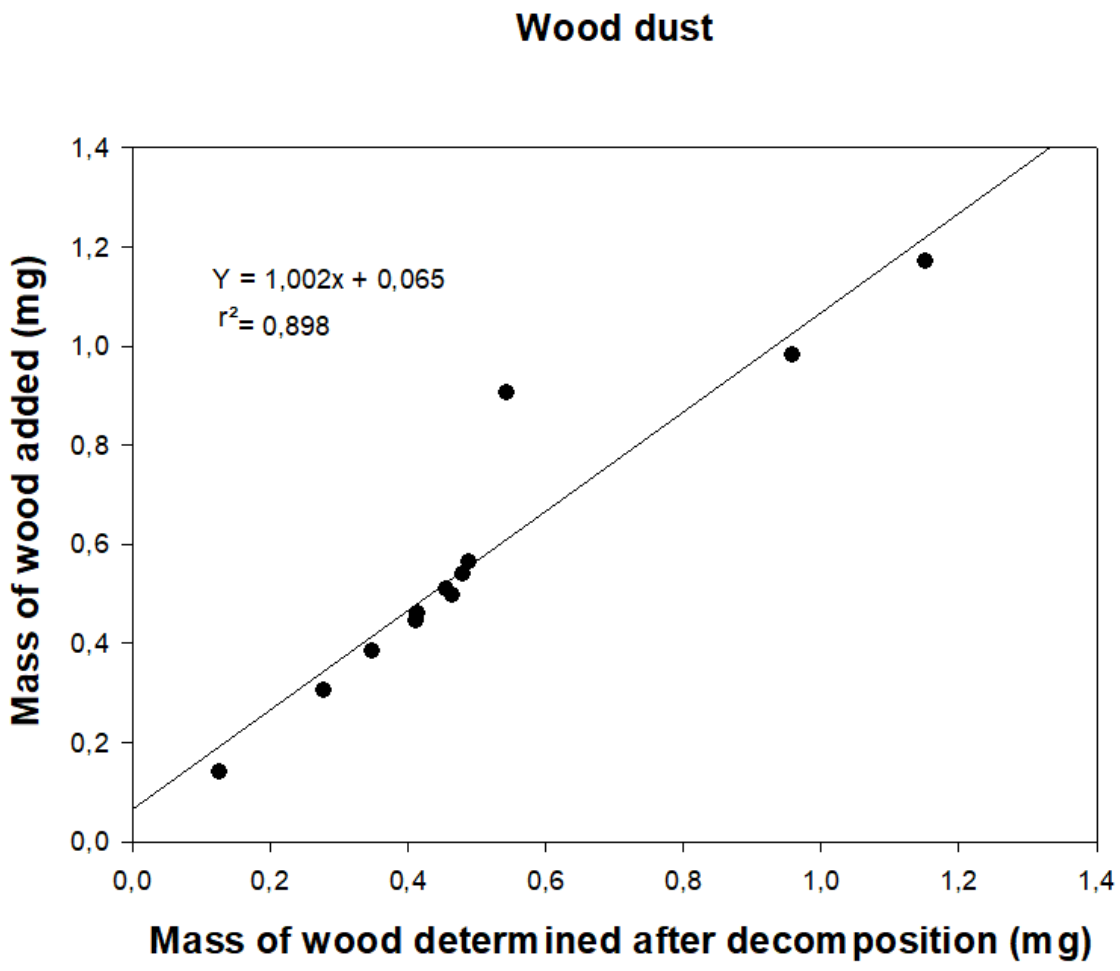

Figure 6: Comparison between loaded mass of wood before and after low plasma thermal decomposition when only wood was present on the filters.

6.2.2 Wood and quartz

6 filters were loaded with wood and quartz, on average 0,767mg of wood dust was added. After decomposition an average of 0,827 mg had been removed, accounting for 105,5% removal of the original added wood dust.

The range of removed mass compared with added wood dust was between 90,8 – 124,4 % for the 6 filters. Figure 7 gives shows the relationship between before and after decomposition. A simple linear regression was performed, the fitted line had the equation 0,083 + 0,828x and the r^2 was reported to 0,954.

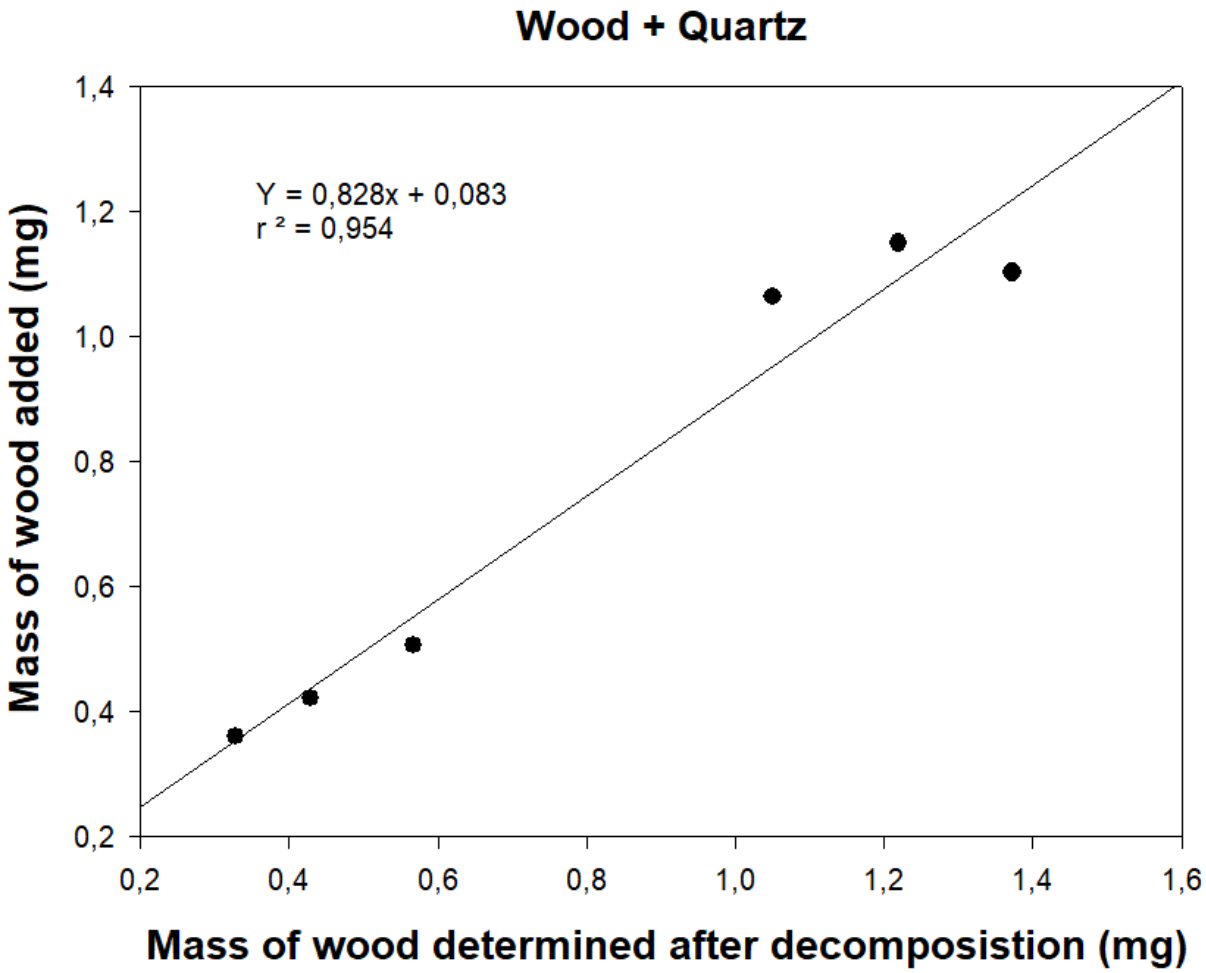

Figure 7: Comparison between loaded mass of wood before and after low plasma thermal decomposition when wood and quartz was present on the filters.

6.2.3 Wood and gypsum

9 filters were loaded with wood and quartz, on average 0,838 mg of wood dust was added. After decomposition an average of 1,942 mg had been removed, accounting for 231,5% removal compared to the original added wood dust.

The range of removed mass compared with added wood dust was between 74,8 – 603,4 % for the 9 filters. Figure 8 gives shows the relationship between before and after decomposition. A simple linear regression was performed, the fitted line had the equation 0,5505 + 0,241x and the r^2 was reported to 0,0510.

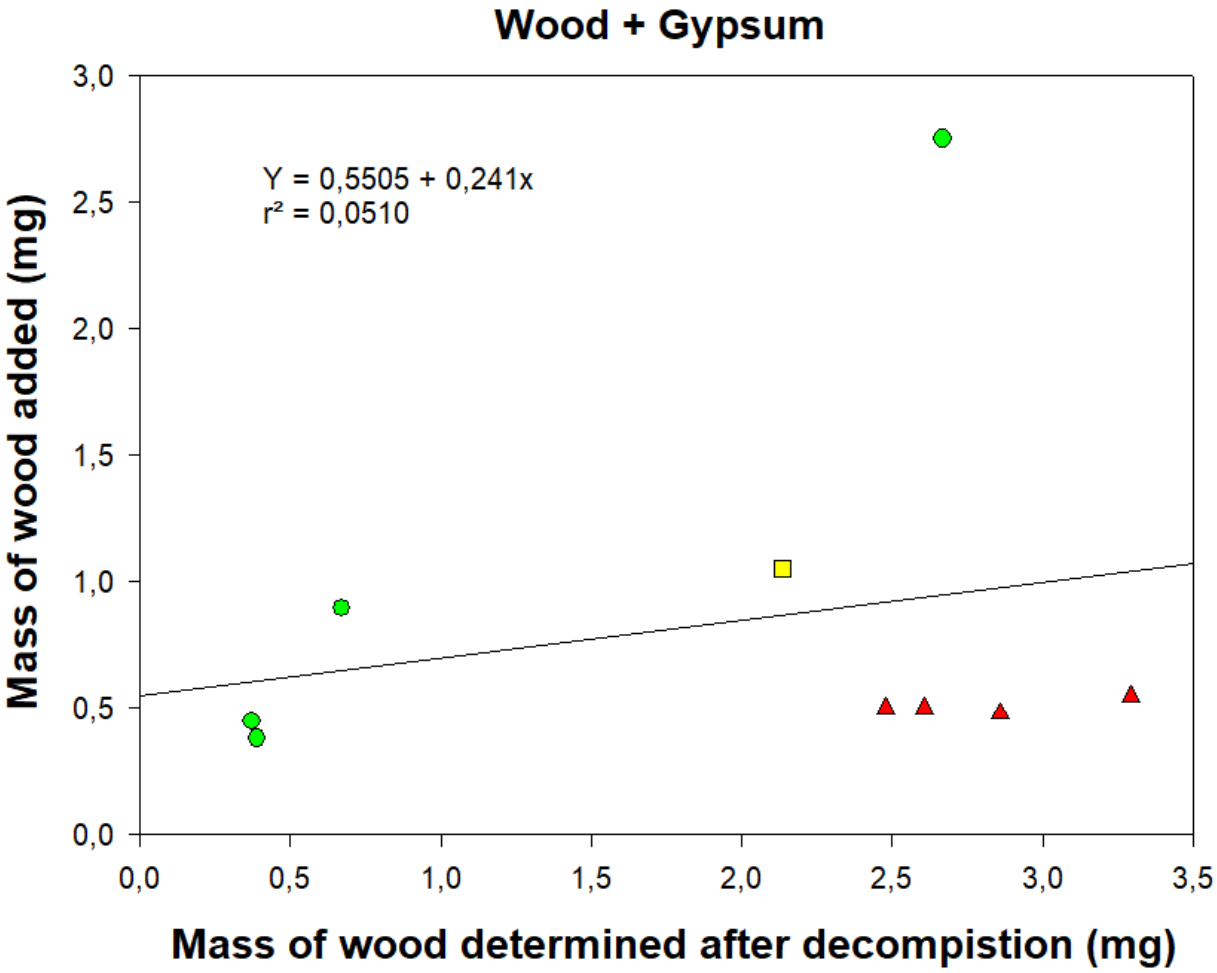

Figure 8: Comparison between loaded mass of wood before and after low plasma thermal decomposition when wood and gypsum was present on the filters. The green colour indicates a loaded mass of gypsum between 0-5 mg, yellow colour indicates loaded mass of gypsum between 5-10mg and red colour indicates loaded mass of gypsum between 10-15mg.

6.2.4 Wood, gypsum, and quartz

10 filters were loaded with wood, gypsum, and quartz, on average 0,833 mg of wood dust was added. After decomposition an average of 1,972 mg had been removed, accounting for 236,5% removal of the original added wood dust.

The range of removed mass compared with added wood dust was between 10,71 – 360,9 % for the 10 filters. Figure 9 gives shows the relationship between before and after decomposition. A simple linear regression was performed, the fitted line had the equation 0,415 + 0,212x and the r^2 was reported to 0,329.

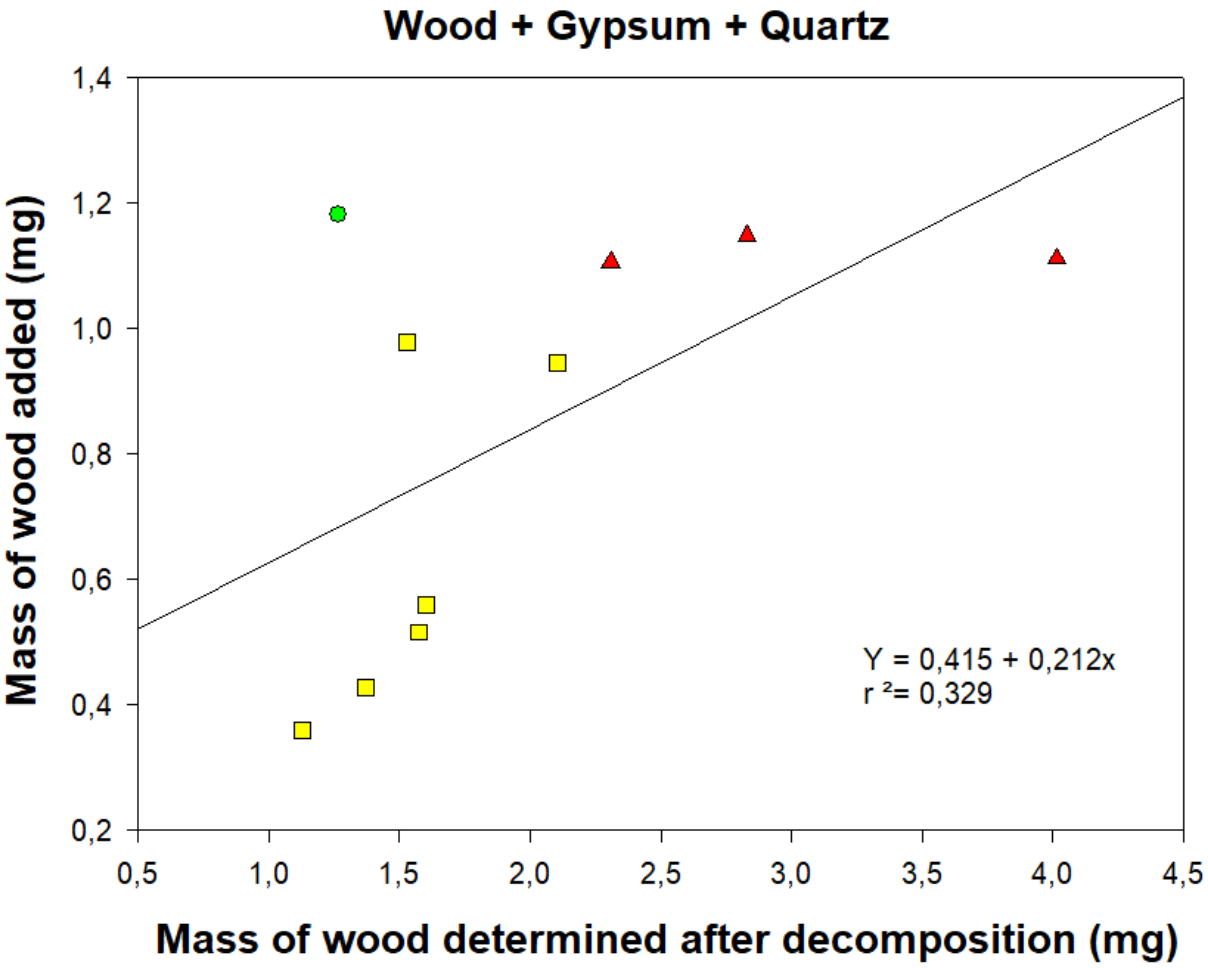

Figure 9: Comparison between loaded mass of wood before and after low plasma thermal decomposition when wood, gypsum and quartz was present on the filters. Green colour indicates a loaded mass of gypsum between 0-5 mg, yellow colour indicates loaded mass of gypsum between 5-10mg, and red colour indicates loaded mass of gypsum between 10-15mg.

6.2.5 Particle size distribution of sanding of wood

APS measurement was done during sanding of wood. Four different aerodynamic diameters between 0,5 – 8,3µ is shown in Figure 10. Of the size presented in Figure 10, 0,5µm and 2,1µm had the highest concentration in the air during the sampling time 10:33 – 12:57. The largest size in figure 10, 8,3 µm, had the lowest concentration in the air during the whole sampling time.

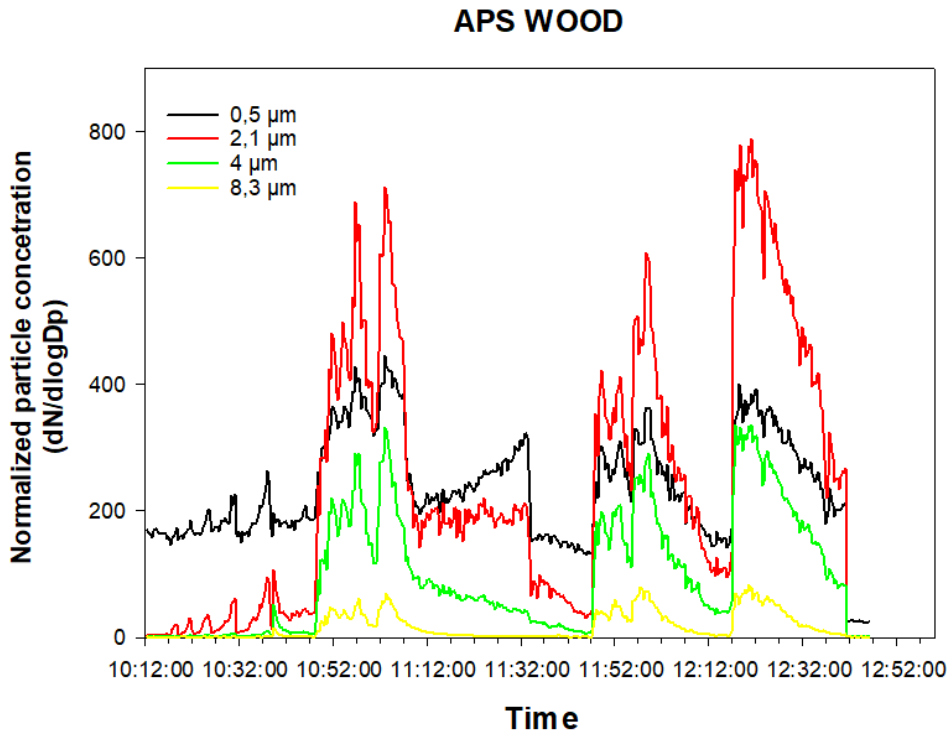

Figure 10: Distribution of four different aerodynamic diameters 0,5, 2,1, 4 and 8,3 µm during sanding of wood at STAM measured with aps.

6.2.6 Particle characterisation for wood

Particles (0.5 to 20 µm) measured by APS inside of tent during grinding of wood. The size distribution in Figure 11 shows the d_{ae} ranged from 0.5 - 16 µm, with peak concentrations approximately at 0.723 µm.

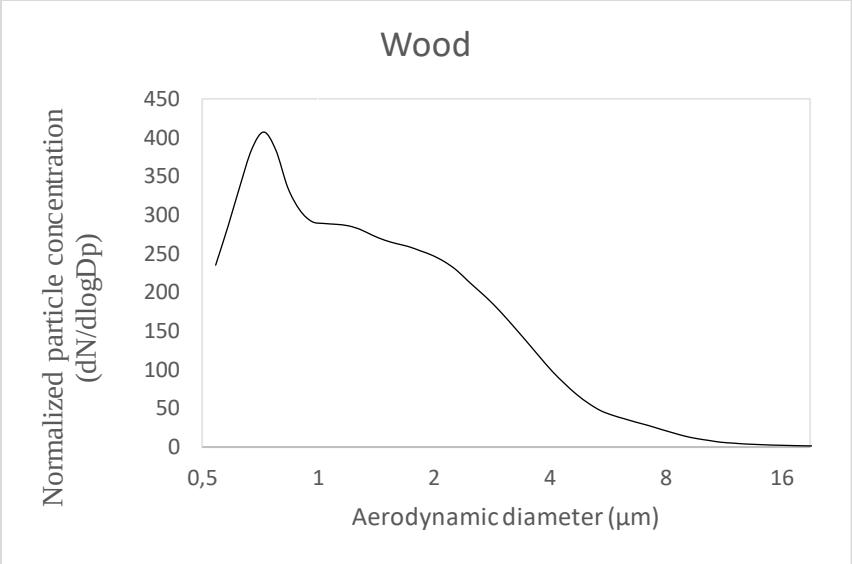

Figure 11: Particle size concentration measured with aps during sanding of wood at STAMI.

6.2.7 Particle size distribution of sanding of gypsum

APS measurement was done during grinding of gypsum. Four different aerodynamic diameters between 0,5 – 8,3µm was shown in figure 12. From the presented d_{ae} in Figure 12, the sizes of 0,5µm and 2,1µm had the highest concentration in the air during the sampling time 10:12 – 12:37. The largest size in figure 16, 8,3 µm, had the lowest concentration in the air during the whole sampling time.

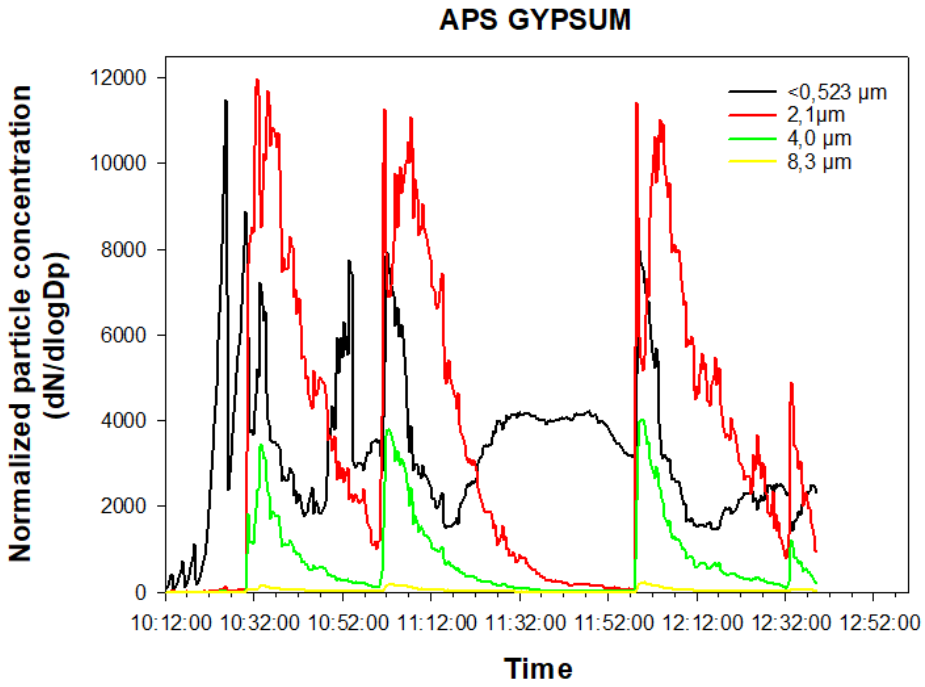

Figure 12: Distribution of four different aerodynamic diameters 0,5, 2,1, 4 and 8,3 µm during sanding of gypsum at STAMI.

6.2.8 Particle characterisation for gypsum

Particles (0.5 to 20 µm) measured by APS inside of tent during grinding of gypsum, showed in figure 13. The size distribution in Figure 13 shows that the d_{ae} ranged from 0.5 µm to 5.05 µm, with peak concentrations at approximately 2,28 µm.

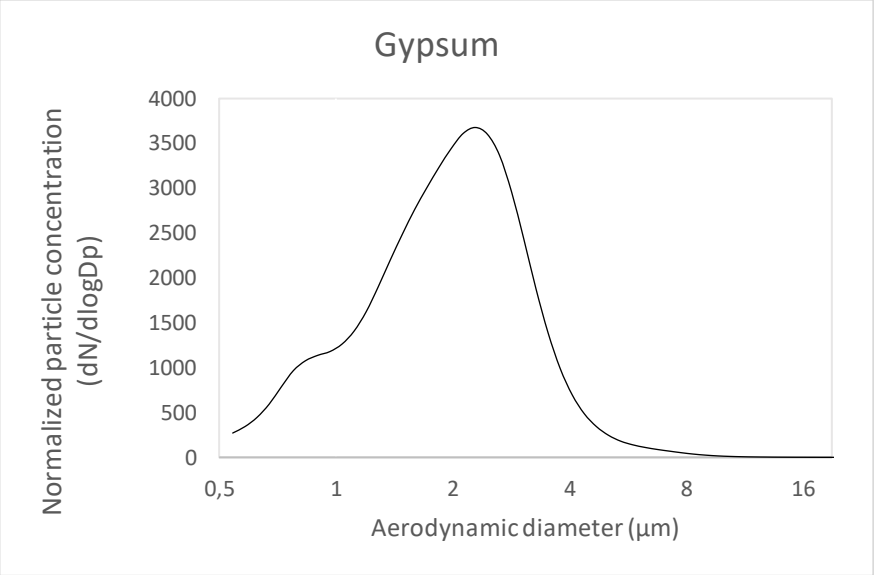

Figure 13: Particle size concentration measured with aps during sanding of gypsum at STAMI.

6.3 Results from construction site

PM was sampled at a construction site in Oslo for both respirable and total dust, shown in Table 2. Respirable dust had AM of 0,378 mg/m^3 day 1 and an AM of 0,450 mg/m^3 day 2. Average estimated organic content after decomposition for collected PM day 1 was 8,95% and 10,66% for day 2. Total dust had AM of 1,06 mg/m^3 day 1 and an AM of 1,03 mg/m^3 day 2. Average estimated organic content after decomposition for collected PM day 1 was 19,25% and 19,26% day 2.

Table 2: Arithmetic mean, geometric mean, standard deviation for collected PM. Average estimated organic content in % after decomposition for both respirable and total dust sampled at construction site. Sampling was divided between 2 days, with 10 samples for both fractions each day.

n=10 samples per day		**Respirable dust (mg/m^3)**			
		AM	GM	STD	Average organic content (%)
Day 1	Collected PM	0,39	0,36	0,12	8,95 %
	Residue PM	0,34	0,33	0,10	
	Estimated organic PM	0,035	0,031	0,019	
Day 2	Collected PM	0,45	0,44	0,11	10,66 %
	Residue PM	0,40	0,39	0,10	
	Estimated organic PM	0,047	0,044	0,021	
		Total dust (mg/m^3)			
		AM	GM	STD	Average organic content (%)
Day 1	Collected PM	1,06	1,04	0,267	19,25%
	Residue PM	0,86	0,84	0,23	
	Estimated organic PM	0,20	0,19	0,067	
Day 2	Collected PM	1,03	0,96	0,38	19,26%
	Residue PM	0,83	0,77	0,31	
	Estimated organic PM	0,20	0,18	0,084	

6.3.1 Particle size concentration from construction site day 1 and day 2

APS measurement was performed during both days when sampling was conducted at the construction site. APS measured continuously during the whole period. Three different aerodynamic diameters between 2,1 – 8,3µm are shown in Figure 14 and 15. Particle concentration from day 2, seemed to be higher than day 1.

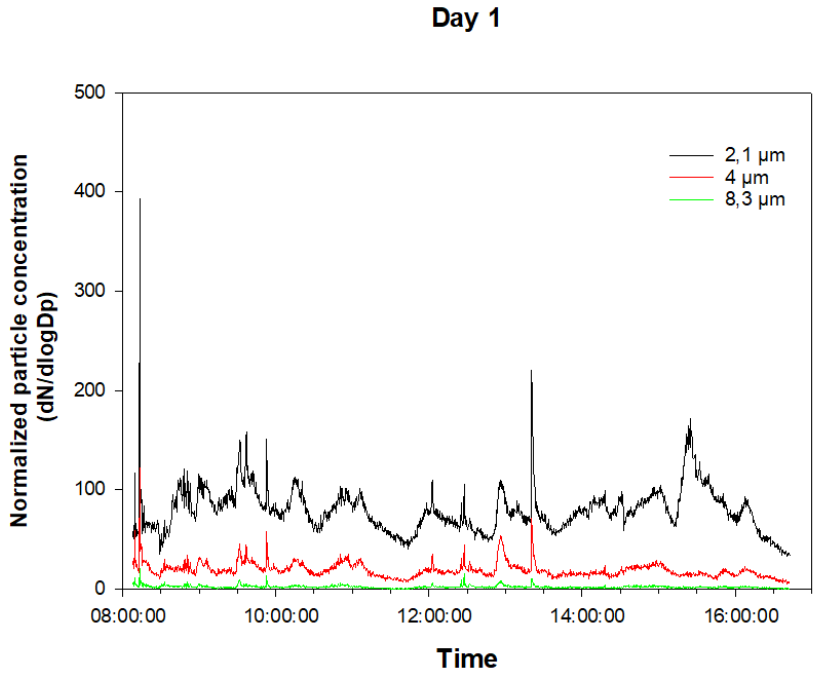

Figure 14: Distribution of three different aerodynamic diameters 2,1, 4 and 8,3 µm as function of time at construction site day 1.

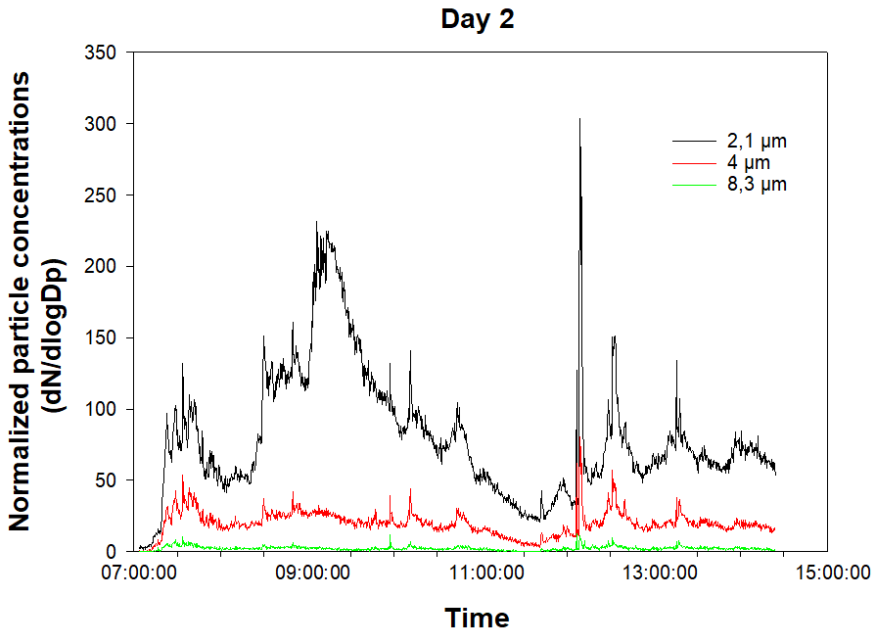

Figure 15: Distribution of three different aerodynamic diameters 2,1, 4 and 8,3 µm as function of time at construction site day 2.

6.3.2 particle characterisation for construction site day 1 and day 2

Particles (0.5 to 20 µm) measured by APS at construction site continuously for two days. The size distribution for the two days were similar and the d_{ae} ranged from 0.5 µm to 15.05 µm, as seen in Figures 16 and 17. For both days the peak concentrations were 0,723 µm. Day 2 had a slightly higher concentration of particles >0,723 µm than day 1.

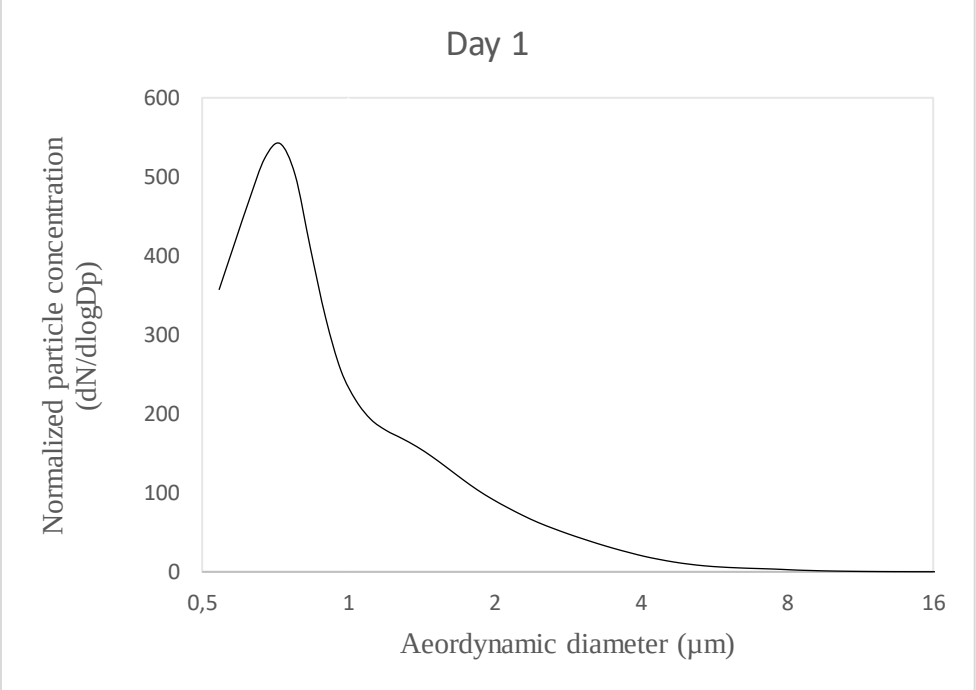

Figure 16: Particle size concentration measured with APS during day 1 from the construction site.

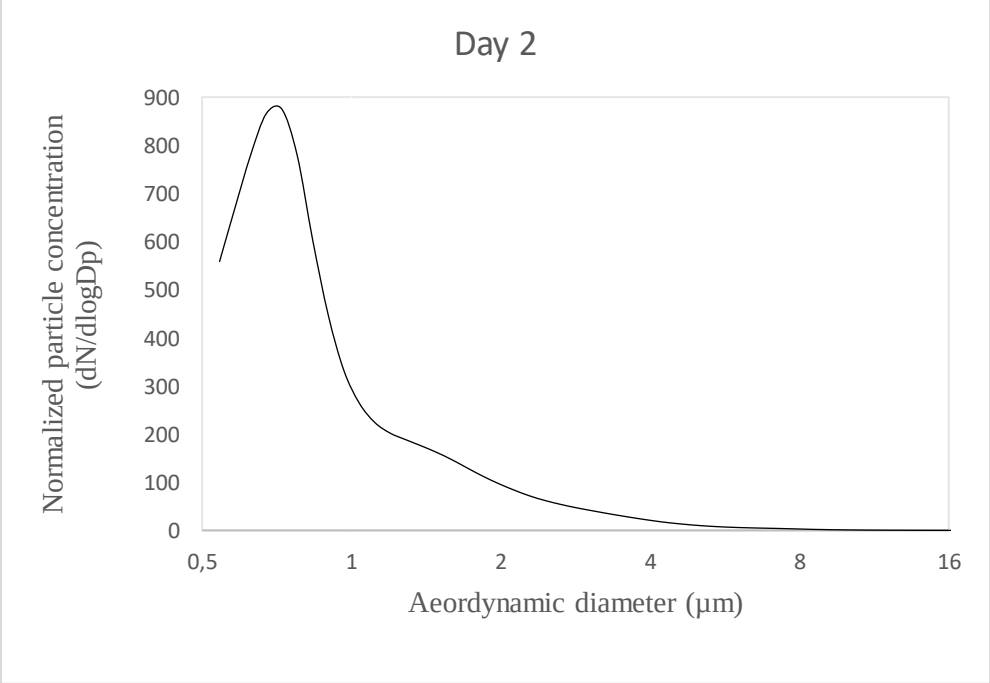

Figure 17: Particle size concentration measured with APS during day 2 from the construction site.

6.3.3 XRD – Results

10 samples from respirable dust day sampled at 1 was examined with XRD by applying the NIOSH Method to measure the content of α-quartz, shown in Table 3. α-quartz was detected at all the 10 filters, the amount varied from 0,0081 – 0,029 mg. The average α-quartz content was 4,5% of the inorganic mass. The α-quartz concentration in the air was between 0,009 – 0,032 mg/m^3. A simple linear regression between residue mass and α-quartz was performed, the reported r^2 was 0,946 and the fitted line was y = 0,106 + 14,99x.

Table 3: α-quartz determined with XRD on respirable dust samples from day 1, residue after decomposition, the percentage of α-quartz in the inorganic residue and the α-quartz (mg/m^3) in the sampled air.

Respirable dust	α-quartz (mg)	α-quartz (%)	α-quartz (mg/m^3)
1	0,010	4,4	0,010
2	0,008	3,3	0,009
3	0,011	4,1	0,012
4	0,012	3,9	0,013
5	0,021	5,3	0,023
6	0,024	5,4	0,026
7	0,016	4,4	0,018
8	0,014	4,8	0,016
9	0,013	4,1	0,015
10	0,029	5,1	0,032

6.3.4 Rietveld analysis of sampled total dust

A Rietveld analysis of 10 total dust samples from the construction site sampled during day 1 was performed. The analysis was done after decomposition of the filters and extraction onto silver filters. The inorganic residue is presented in Table 4, these consisted of the minerals: calcite, alite, quarts, feldspar, illite/smectite and biotite. Calcite, quartz, feldspar, and biotite was present at all the filters. Four filters had alite present and six filters had illite/smectite present. Calcite averaged (AM) at 57 % of the mass, quartz at 12 %, feldspar at 23% and biotite at 3,6 %. For the filters with alite and illite/smectite the average was 10% and 3,4 % of the mass.

Table 4: Rietveld analysis of the composition (%) of PM collected from total dust at construction site day 1. Analysis was done after decomposition of the total dust samples.

Total dust samples	Calcite	Alite	Quartz	Feldspar	Illite/Smectite (clay mineral)	Biotite (mica)
1	46 %	0 %	16 %	31 %	1,0 %	7,3 %
2	70 %	0 %	11 %	15 %	0,0 %	4,8 %
3	61 %	0 %	11 %	25 %	0,0 %	3,0 %
4	54 %	11 %	12 %	24 %	4,0 %	2,0 %
5	54 %	0 %	13 %	26 %	5,0 %	1,0 %
6	57 %	0 %	13 %	25 %	3,5 %	2,2 %
7	56 %	6 %	14 %	17 %	0,0 %	7,0 %
8	47 %	11 %	13 %	26 %	0,3 %	4,0 %
9	53 %	0 %	11 %	26 %	6,4 %	3,8 %
10	70 %	11 %	7 %	10 %	0,0 %	0,7 %

Table 5, overview of the mass distribution (mg/m^3) after correction of removed organic content. Calcite averaged at 0,49 mg/m^3, Alite 0,033 mg/m^3, Quartz 0,10 mg/m^3, Feldspar 0,19 mg/m^3, Illite/smectite 0,017 mg/m^3 and Biotite 0,031 mg/m^3.

Table 5: The different amounts of minerals (mg/m^3) in the collected PM for total dust, corrected for the loss of organic content day 1.

Total dust samples	Calcite (mg/m^3)	Alite (mg/m^3)	Quartz (mg/m^3)	Feldspar (mg/m^3)	Illite/Smectite (mg/m^3)	Biotite (mg/m^3)
1	0,39	0,00	0,14	0,27	0,01	0,06
2	0,60	0,00	0,09	0,13	0,00	0,04
3	0,52	0,00	0,09	0,21	0,00	0,03
4	0,46	0,09	0,10	0,21	0,03	0,02
5	0,46	0,00	0,11	0,22	0,04	0,01
6	0,49	0,00	0,11	0,21	0,03	0,02
7	0,48	0,05	0,12	0,15	0,00	0,06
8	0,40	0,09	0,11	0,22	0,00	0,03
9	0,46	0,00	0,09	0,22	0,05	0,03
10	0,60	0,09	0,06	0,09	0,00	0,01

6.3.5 SEM-EDS analysis of sampled total dust

A few collected samples from construction site were after decomposition and extraction examined with SEM to better understand the components constituting the PM at the site. SEM-EDS mapping was used to produce a high-resolution element map. The elements were displayed in different colour to distinguish them. Figures 18 and 19 was from the same sample of collected total dust. In Figure 18, two elements in the mapping were shown, calcium and silicon. Calcium rich particles (red) was not seen in combination with silicon (blue).

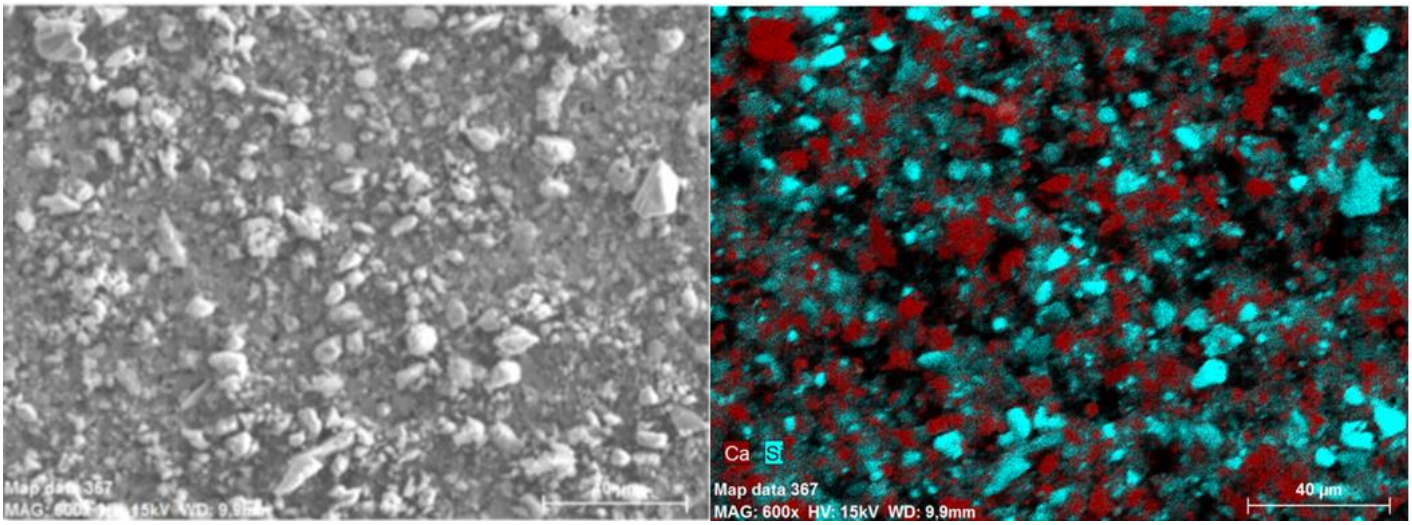

Figure 18: Picture to the left, secondary electron image of collected particles on the Ag filter magnified 600x, picture to right SEM-EDS mapping on the particles, Ca (red) and Si (blue)

Five elements are shown in Figure 19, silicon, iron, aluminium, carbon, and sulphur. Silicon particles (red) was present in combination with aluminium (orange), iron (yellow) seen as spherical particle. Sulphur (purple) was present in the crystal and carbon rich particles shown as green.

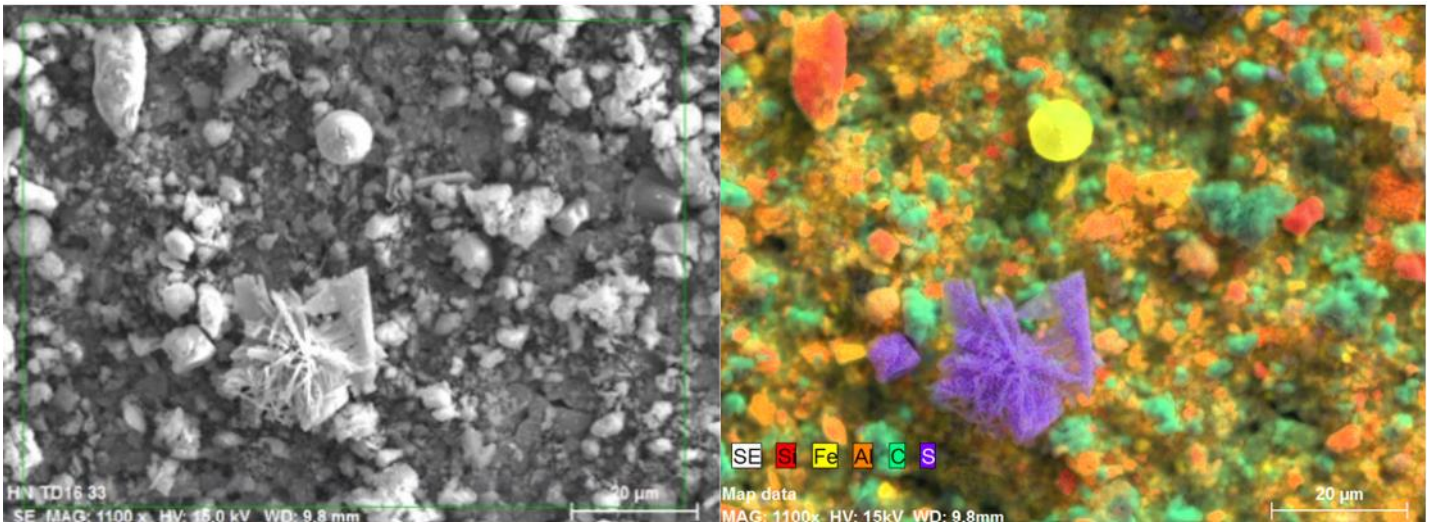

Figure 19: Picture to the left, secondary electron image of collected particles on the Ag filter magnified 1100x, picture to right SEM-EDS mapping on the particles, Si(red), Fe(yellow), Al(orange), C (green) and S(purple).

7.0 Discussion

7.1 Experimental sampling setup

The aim with the experimental set up was to collect PM from wood and gypsum. To simplify the sampling, it was decided to use a tent, where work could be conducted. The tent used was applied from STAMI. The total size was 4 x 3m and it was erected in the backyard at the offices to STAMI. An interior wall was put up inside, limiting the working area to a size of 2,5 x 2,5m. Production of PM from wood proved to be manageable. Sanding of wood produced considerable amounts of dust. This could be seen from the airborne particle concentrations measured inside the tent in Figure 10. The measurements showed high concentration of the sizes 0,5, 2,1 and 4,0 µm. Wood has been reported be in the sizes of around 10 µm. The 10 µm size is connected to the work being inflicted to the wood, particularly sawing. In the case of sanding, smaller particles were emitted, thereby it made sense that smaller particles were suspended in the air. Particle characterisation, as seen in figure 11, also indicates that the smaller sizes were the most prevalent in the air.

The sanding of gypsum boards produced a lot of PM in a short amount of time. Gypsum is a brittle and porous material, in comparison to wood, and this was probably the reason why more visible dust was generated. As for wood, the largest particles concentration in Figure 12, was the sizes 0,5, 2,1 and 4,0 µm. Comparison of particle size characterisation in Figure 11 and 13, showed that the median size of the gypsum particles was bigger than those for wood. Nevertheless, the size distribution of the wood particles shows a longer tail, indicating that larger particles were generated. In this case it shouldn't had any implications on the sampling since total dust samplers generally samples all size up 40 µm d_{ae}. This meant that similar sizes for both wood and gypsum were sampled.

There was evidence that the amount of PM had have overloaded the PVC filters. Opening cassettes after sampling to determine collected mass, almost all the filters had a layer on top with gypsum who easily fell off. This was not the case when sampling wood dust, there wasn't anything that fell visibly off when handling the filters.

A drawback with this setup was the lack of control. Collection of the different compounds varied, there was little consistency in the mass sampled. In Table 1, an overview of the different combinations and added masses are presented. Gypsum had the highest average loading range on the filters, between 6,5 - 7,7 mg. In comparison wood had an average loading of 0,575 – 0,838mg. When wood and gypsum or wood, quartz and gypsum were present in combination, gypsum was the biggest contributor to the total mass. Variation

between loaded masses were high and there was little consistency in the amount deposited due the method. The inconsistency seen in collected masses demonstrated in Table 1, may have had an impact on the results after decomposition.

Concentration of PM in the air inside the tent was higher than those collected from the construction site. Furthermore, the tent was not airtight, there was also a possibility that PM from surrounding area could have been mixed into the air inside the tent and sampled other compounds than wood and gypsum. The work was done during two days in February, working during the winter period meant that the temperature outside was sub-zero and the ground was covered in a thin layer of snow. Therefore, several conditions were not possible to control, e.g temperature, moisture.

7.2 Materials used in the experimental sampling setup

The wood and gypsum materials where residue materials from STAMI. The wood was from a wooden pallet, usually called a "EUROPAL". It had been laying outside and had some signs of weathering. The wood was not analyzed, but it was assumed it was of a Nordic soft type (spruce or pine) and that no treatment or chemicals had been applied.

Using a pallet was out of practical consideration and availability. The idea was not to have "analytical grade" wood, but something similar to what could be found in "real" life. Construction sites are messy and unclean, materials lay around in the open, being exposed to various contaminations from surrounding environment. The pallet used was a good representation of wooden materials used at building sites.

The gypsum also came from a residue, it was a gypsum board who was covered with a layer cardboard. The carboard was removed before sanding. The board didn't have any sign of weathering, it had been laying inside. The composition of the gypsum board was not analyzed, but it was assumed that it consisted mainly of $CaSO_4 * 2H_2O$.

Quartz was added directly onto the filters, the quartz was α – quartz, obtained from a standardize reference material. It was decided not sampled it in same ways as gypsum and wood. This was because working with materials with a high quartz content would have been labour intensive and required specialized tools and protection. The quartz portion was the only analytical grade material added.

7.3 Low temperature plasma decomposition

LTP was used instead of thermal decomposition to remove filter substrate and decompose organic materials deposited. In comparison to thermal decomposition, where temperatures can be as high as 500-600°C, low temperature plasma is based on ionized O_2 gas at temperatures ~ 120 °C. The idea of using this method, was to reduce the need for correction after decomposition. With a lower temperature, there should not be any need for correction of the gypsum. Gypsum converts into lime at about 600°C and the dehydration of gypsum take place around 200°C (Stacey et al., 2019). Furthermore, the low temperature minimizes the risk of altering any structure characterizing (3-D structures).

Residue of filters and wood seemed to be removed without any loss of inorganic materials collected onto the filters. Filters with only containing wood dust, had no or little mass left indicating that most of the organic material had been combusted in the procedure. The residue from the blank filters was insignificant for the overall results.

7.4 Results after decomposition

One of the aims of the thesis was to better estimate the proportion of dust collected onto filters. Currently these are only based on gravimetrical decision of one component, making it hard to distinguish what is sampled. With the inhouse prepared samples, the goal was to see if the decomposition procedure removed organic content and determine the inorganic fractions.

To investigate the accuracy of the decomposition of organic fractions, only wood dust was added to the filters. Mass of wood before the low temperature decomposition was on average 0,575 mg, after LTA the average removal was 88,5 %. An indication there was a portion of the wood that wasn't removed. Figure 6 showed the relationship between the mass of wood before decomposition and estimated amount decomposed based on residue weight after the procedure. The figure demonstrates that most results, for test samples of total dust on PVC filters subjected to decomposition procedure were close to the expected mass of wood (slope = 1.002). From the fitted line, the r^2 value of 0,898 was, further indicating at reasonable correlation between the masses before and after, when no other components were present.

The results varied when other compounds were added. For the combination of wood and gypsum the average removal was 231,5 % compared to original mass of wood added before decomposition. The range of removal was not consistent, for the 9 filters the removal rate was between 74,8 – 603,4%. The fitted line had a reported r^2 value of 0,0511, this was the lowest

value for all the combinations, but it was not surprising due the inconsistencies from the results. The variation, due to lost masses was shown in Figure 8. The colours in Figure 8 indicate the amount of gypsum added to each filter. From the figure, the largest amount of gypsum added had the highest differences before and after decomposition. Where the amount of gypsum was low, the difference between loaded mass and collected residue was more accurate. It was unlikely that the loss or altering of the gypsum was because of decomposition procedure, because of the low temperature used in the process. Losses of gypsum was more likely connected to the different steps undertaken when measured and extracted.

The combination of wood and quartz was more promising than to the combination of gypsum and wood. After decomposition 107,7 % was removed compared to original mass of wood added, this was even result in percentage than when wood was the only added fraction. In comparison to the gypsum, a relatively low mass of quartz was added, this meant that less mass could be lost in during weighing and extraction process after decomposition. The results from the combination of wood and quartz also implies that quartz was not affected by the decomposition procedure. As seen in Figure 7, the r^2 value from the fitted line was 0,9546, this was the highest r^2 value of all the combinations from the prepared samples.

The combination with all three components: wood, gypsum and quartz had the biggest difference between added masses and removed masses after decomposition. An average of 236, 6 % was removed, compared to the original mass of wood added. As seen with the combination for wood and gypsum, the removal rate varied, with removed masses between 107,1 – 360,9%. The high removal of masses was similar in percentage to the combination of wood and gypsum. Indication of that the gypsum was an important contributor to the mass loss as seen in both cases. The r^2 value from the fitted line in Figure 9 was 0,329, this was higher than the r^2 value from the wood and gypsum. It was likely higher because of the higher average total mass added to the filters compared to the average for the wood and gypsum combination.

7.5 Field samples from construction sites

Two types of size fractions were sampled on the construction site during the two sampling days, respirable and total dust. Collected PM was highest for total dust both days, with an average mass concentration of 1,06 mg/m^3 day 1 and 1,03 mg/m^3 day 2. Between these two days there was little difference in the collected amount. Indicating similar conditions both days regarding the total dust fraction at the site.

The difference in the respirable size fraction between the two days was larger, averaging 0,378 mg/m^3 for day 1 and 0,450 mg/m^3 for day 2. The APS measured a higher particle number concentration in day 2, as seen in Figure 15 compared to day 1, as seen in Figure 14. The size distribution curve seen in Figure 17 was similar both days, indicating similar dust. However, higher concentration of smaller particles for day 2 can be seen in Figure 17. This might explain the variances between the two days in sampled mass. It should be noted that the largest wood dust particles may have been missed by the APS, as it was positioned some meters from the work operations. The largest particles may have settled before reaching the APS.

After decomposition the average lost mass for the total dust filters were 19,25 % day 1 and 19,26 % day 2. The organic matter removed may be a mixture of wood dust, fungal spores, cellulose fibres, pollen etc. Since woodwork was taking place in the sampling area, it is reasonable to believe that a larger share of the organic dust was wood dust. This meant that nearly 80% of the collected PM sampled consisted of a mixture of different inorganic materials. With the current gravimetrical approach, a calculation would have overestimated the amount of wood dust present in the air. The results after decomposition indicated that PM on a construction site had a complex mixture.

10 samples from the total dust sampled at construction site day was analysed with XRD after decomposition. The Rietveld method was applied to characterize and quantify the crystalline materials. The minerals found by the Rietveld method is presented in Table 4. Calcite was the highest contributor to mass and accounted on average for 57% of the inorganic residue. The mapping with SEM – EDS in Figure 18 and 19 also showed that several of the particles were calcium and carbon rich particles. In Figure 19 the crystal-like structure contained sulphur in combination with calcium. The particle was likely gypsum ($CaSO_4$). The carbon didn't look as it was present with other elements, but the presence might indicate calcium carbonate ($CaCO_3$). In figure 18, calcium rich particles didn't derive from minerals containing silica, but might be from calcium oxide (CaO). The silicon particles seen in Figures 18 and 19 were most likely from minerals as biotite, quartz and feldspar.

The large amount of calcite was likely due to the carbonation process of calcium oxide to calcite in the concrete. Silicon containing minerals such as quartz, feldspar and biotite was present at all the filters. The SEM – EDS mapping proved that many silicon rich particles often consisted of aluminium. Quartz, feldspar types and biotite are found in sand and gravel are therefore also like from the concrete or from mortar used in between bricks. Some clay minerals were found

and may originate from bricks. Furthermore, elements as iron and sulphur were observed in some particles. The presence of both sulphur and calcium was an indication that there was also gypsum in the air at the construction site. The iron rich particles may be an iron oxide particle. Gypsum and iron oxide were not found by the Rietveld method. Most likely the prevalence of these compounds was not significant. Nevertheless, the SEM – EDS mapping illustrates the complex mixture of particles present.

Estimation of the α-quartz concentration in the total dust was on average 0,10 mg/m^3 after correction of removed organic content, as seen in Table 5. This was lower than the current Norwegian OEL of 0,3mg/m^3. Even if the values for α-quartz was lower than the limit of 0,03mg/m^3. It showed that only measuring one fraction is not a good approach to estimate the exposure of workers, especially at construction sites where rehabilitation is being undertaken.

For the respirable dust, the loss of mass after decomposition was on average 8,95 % for day 1 and on average 10,66 % for day 2 for the collected mass, presented in Table 2. The lower organic mass can be due to the cut off at samplers. Wood particles are usually bigger, with particles being around 10µm when cutting and sawing is performed, slightly bigger than the cut-off for the respirable fraction. With the assumption that all organic material was removed, approximately 90% of the collected PM was from other sources than organic origin, in this case, the smallest fractions consisted of inorganic material.

10 samples of the respirable dust from day 1 was examined with XRD to determine the α – quartz content, as shown in Table 3. The α-quartz was present in all the samples and accounted for 3,3 – 5,4 % of the mass in the inorganic residue. The variation of quartz content seemed to be connected to the amount of collected mass. Estimation of α-quartz in mg/m^3 was between 0,009 – 0,032. This meant that all the 10 samples had values of respirable quartz lower than the OEL of 0,05mg/m^3. As for the total dust samples, the quartz content was below appointed OELs, which was positive regarding exposure for the workers. No Rietveld or SEM – EDS mapping was performed on the respirable dust, but the elemental and mineral composition as seen for total dust samples were likely similar due to the sampling method.

7.6 Limitations of the work

There were several limitations to the work undertaken in this thesis. Recreation of the setup might be difficult, due the limitations stated in the discussion, and since this procedure is not based on any current standardisation. Furthermore, the materials used for wood and gypsum was not standardized reference materials, and there was likely contamination of other inorganic substances that might have contributed to sampled mass.

A factor that that influenced the results was the preparations and handling of the filters. The filters, particularly those made at STAMI were weighed several times to determine loaded masses added during the sampling procedure. Placed inside cassettes these had to be opened between sampling and loading of the different fractions. Removal of the filters from the cassettes was difficult without losing mass. With gypsum present it was challenging to not lose some of the collected mass as the filters were removed, weighed, and assembled back into the cassettes. Evidence could be seen with residue on the weight after measuring and with gypsum falling off when removing filters from the cassettes.

The extraction process was also a step who accounted for uncertainty, with gypsum a lot of residues wasn't deposited onto the silver filters. The inclusion of all the different steps added a lot of insecurity to the results.

8.0 Conclusion

The results in this thesis aligns with the hypothesis that a low thermal plasma based gravimetric approach would increases accuracy when measuring wood dust in complex air samples. The approach did give better estimation of wood dust in complex air samples. For the inhouse prepared samples, the method did remove wood dust. The accuracy of determining the wood dust content varied with the different combinations. When only wood was added, the estimation of wood dust after the procedure were similar with the added amount. The same results were also seen for the combination of the wood and quartz, with a good match for the amount added of wood before and residue after decomposition.

When gypsum was present, there was large a variation in the estimation of wood dust content. The mass of wood based on mass loss was several times higher than original mass of wood added. As gypsum should not be affected by the low temperatures decomposition this was unexpected. However, the highest loss of mass after decomposition was in the samples with high mass of gypsum. This might be due to the laborious analytical process, which included repeated weighing and successive transfer of filters to collect the different types of dust. An indication that it might not be the decomposition that affected the results.

The results from construction site showed that wood dust was not the biggest contributor to PM in the air. In the respirable fraction, it was estimated that the organic material only accounted for approximately 10% of the overall weight. This meant that 90% had a mixture of inorganic material with different composition. For the total dust, the estimated removed organic matter after decomposition accounted for approximately 19% of the mass. Only relying on gravimetrical measurement in complex air samples without decomposition would have overestimated the amount of wood in the working air. The low thermal plasma decomposition improved the determination of wood dust, if it's assumed that all the organic matter removed was only consisting of wood. The approach in this thesis shows that applying a decomposition step was an important tool to better understand the PM in air samples from rehabilitation sites in construction.

Combining the decomposition step with SEM-EDS, XRD and the Rietveld method was a useful approach to quantitatively describe the mixed exposure. These analytical tools revealed that PM in the air consisted of a mixture of several different minerals and elements. It gave a better understanding of the complex exposure that construction workers are exposed to at rehabilitation sites and that these are dominated by inorganic fractions.

References

Adamovich, I., Baalrud, S. D., Bogaerts, A., Bruggeman, P. J., Cappelli, M., Colombo, V., Czarnetzki, U., Ebert, U., Eden, J. G., & Favia, P. (2017). The 2017 Plasma Roadmap: Low temperature plasma science and technology. *Journal of Physics D: Applied Physics*, *50*(32), 323001.

Arbeidstilsynet. (2021a). Grenseverdier for kjemisk eksponering. Available at: https://www.arbeidstilsynet.no/tema/kjemikalier/grenseverdier-for-kjemisk-pavirking/ (accessed: 12.02).

Baran, S., & Teul, I. (2007). *WOOD DUST: AN OCCUPATIONAL HAZARD WHICH INCREASES THE RISK OF RESPIRATORY DISEASE*.

Baron, P. A., Rice, F. L., Key-Schwartz, R., Bartley, D., & Schlecht, P. (2002). *Health effects of occupational exposure to respirable crystalline silica*.

Brendstrup, T., Hasle, P., Jensen, E., Nielsen, H., Silberschmid, M., & Vendelbo, O. (1990). The risk of silicosis from building site dust. *Ugeskrift for Laeger*, *152*(26), 1882–1886.

Brown, J. S., Gordon, T., Price, O., & Asgharian, B. (2013). Thoracic and respirable particle definitions for human health risk assessment. *Particle and Fibre Toxicology*, *10*(1), 12. https://doi.org/10.1186/1743-8977-10-12

Cancer, I. A. for R. on. (1987). Monographs on the evaluation of carcinogenic risk to humans, supplement 7. *http://monographs. iarc. fr/ENG/Monographs/suppl7/suppl7. pdf*.

CEN, E. (1993). *481.(1993) Workplace Atmospheres. Size Fraction Definitions for Measurement of Airborne Particles*. European Committee for Standardization, Brussels, Belgium.

Cheriyan, D., & Choi, J. (2020). A review of research on particulate matter pollution in the construction industry. *Journal of Cleaner Production*, *254*, 120077. https://doi.org/10.1016/j.jclepro.2020.120077

Frumkin, H. (Red.). (2016). *Environmental health: From global to local* (Third edition). Jossey-Bass, A Wiley Brand.

Hafner, B. (2007). Scanning electron microscopy primer. *Characterization Facility, University of Minnesota-Twin Cities*, 1–29.

Humans, I. W. G. on the E. of C. R. to. (2012). SILICA DUST, CRYSTALLINE, IN THE FORM OF QUARTZ OR CRISTOBALITE. I *Arsenic, Metals, Fibres and Dusts*. International Agency for Research on Cancer. https://www.ncbi.nlm.nih.gov/books/NBK304370/

Hygienists, A. C. of G. I. (2004). *2004 TLVs and BEIs: Based on the Documentation of the Threshold Limit Values for Chemical Substances and Physical Agents & Biological Exposure Indices*.

Jiménez, A. S., van Tongeren, M., & Cherrie, J. W. (u.å.). *A review of monitoring methods for inhalable hardwood dust*.

Johnston, J. R. (2000). Hazard Prevention and Control in the Work Environment: Airborne Dust. Protection of the Human Environment Occupational Health and Environmental Health Series, Geneva, 1999, World Health Organization WHO/SDE/OEH/99.14: English only. *Annals of Occupational Hygiene*, *44*(5), 405–405.

Karni, J., & Karni, E. (1995). Gypsum in construction: Origin and properties. *Materials and Structures*, *28*(2), 92–100. https://doi.org/10.1007/BF02473176

Kirkeskov, L., Hanskov, D. J. A., & Brauer, C. (2016). Total and respirable dust exposures among carpenters and demolition workers during indoor work in Denmark. *Journal of Occupational Medicine and Toxicology*, *11*(1), 45. https://doi.org/10.1186/s12995-016-0134-5

Moore, E., & Smart, L. (2021). *Solid state chemistry: An introduction* (Fifth edition). CRC Press.

Nasrollahzadeh, M., Atarod, M., Sajjadi, M., Sajadi, S. M., & Issaabadi, Z. (2019). Plant-Mediated Green Synthesis of Nanostructures: Mechanisms, Characterization, and Applications. I *Interface Science and Technology* (Bd. 28, s. 199–322). Elsevier. https://doi.org/10.1016/B978-0-12-813586-0.00006-7

NIOSH hazard review: Health effects of occupational exposure to respirable crystalline silica. (2002). U.S. Department of Health and Human Services, Public Health Service, Centers for Disease Control and Prevention, National Institute for Occupational Safety and Health. https://doi.org/10.26616/NIOSHPUB2002129

NOA (2021). Fakta om arbeidsmiljøet i byggebransjen. Arbeidsmiljøportalen. Available at: https://www.arbeidsmiljoportalen.no/bransje/bygg/fakta-om-bransjen. (accessed: 14.01)

Næringenes økonomiske utvikling. (2022). SSB. Available at https://www.ssb.no/virksomheter-foretak-og-regnskap/virksomheter-og-foretak/statistikk/naeringenes-okonomiske-utvikling(accessed 23.01)

Qi, C., Echt, A., & Gressel, M. G. (2016). On the Characterization of the Generation Rate and Size-Dependent Crystalline Silica Content of the Dust from Cutting Fiber Cement Siding. *The Annals of Occupational Hygiene*, *60*(2), 220–230. https://doi.org/10.1093/annhyg/mev066

Runčevski, T., & Brown, C. M. (2021). The Rietveld Refinement Method: Half of a Century Anniversary. *Crystal Growth & Design*, *21*(9), 4821–4822. https://doi.org/10.1021/acs.cgd.1c00854

Schenk, L., Hansson, S. O., Rudén, C., & Gilek, M. (2008). Occupational exposure limits: A comparative study. *Regulatory toxicology and pharmacology*, *50*(2), 261–270.

SCOEL. (2003). *Recommendation from the scientific committee on occupational exposure limits: Risk assessment for wood dust*. European Commission, Employment and Social Affairs DG Luxemburg.

Sevilla, P., Lopez-Suarez, C., Pelaez, J., Tobar, C., Rodriguez-Alonso, V., & Suarez, M. J. (2020). Influence of Low-Pressure Plasma on the Surface Properties of CAD-CAM Leucite-Reinforced Feldspar and Resin Matrix Ceramics. *Applied Sciences*, *10*(24), Artikkel 24. https://doi.org/10.3390/app10248856

Shepherd, S., Woskie, S. R., Holcroft, C., & Ellenbecker, M. (2008). Reducing silica and dust exposures in construction during use of powered concrete-cutting hand tools: Efficacy of local exhaust ventilation on hammer drills. *Journal of occupational and environmental hygiene*, *6*(1), 42–51.

Shtraichman, O., Blanc, P. D., Ollech, J. E., Fridel, L., Fuks, L., Fireman, E., & Kramer, M. R. (2015). Outbreak of autoimmune disease in silicosis linked to artificial stone. *Occupational Medicine*, *65*(6), 444–450. https://doi.org/10.1093/occmed/kqv073

Sirianni, G., Hosgood III, H. D., Slade, M. D., & Borak, J. (2008). Particle size distribution and particle size-related crystalline silica content in granite quarry dust. *Journal of occupational and environmental hygiene*, *5*(5), 279–285.

Stacey, P., Simpson, A., & Hambling, S. (2019). The Measurement of Wood in Construction Dust Samples: A Furnace Based Thermal Gravimetric Approach. *Annals of Work Exposures and Health*, *63*(9), 1070–1080. https://doi.org/10.1093/annweh/wxz072

Tatum, V. L., Ray, A. E., & Rovell-Rixx, D. C. (2001). The Performance of Personal Inhalable Dust Samplers in Wood-Products Industry Facilities. *Applied Occupational and Environmental Hygiene*, *16*(7), 763–769. https://doi.org/10.1080/10473220121612

Vacuum | Definition & Facts | Britannica. (n.d). Available at: https://www.britannica.com/science/vacuum-physics (accessed: 23.03)

Vardelle, A., Moreau, C., Akedo, J., Ashrafizadeh, H., Berndt, C. C., Berghaus, J. O., Boulos, M., Brogan, J., Bourtsalas, A. C., Dolatabadi, A., Dorfman, M., Eden, T. J., Fauchais, P., Fisher, G., Gaertner, F., Gindrat, M., Henne, R., Hyland, M., Irissou, E., … Vuoristo, P. (2016). The 2016 Thermal Spray Roadmap. *Journal of Thermal Spray Technology*, *25*(8), 1376–1440. https://doi.org/10.1007/s11666-016-0473-x

Vincent, J. H. (2007). *Aerosol sampling: Science, standards, instrumentation and applications*. John Wiley & Sons.

Wang, M., Yao, G., Sun, Y., Yang, Y., & Deng, R. (2023). Exposure to construction dust and health impacts – A review. *Chemosphere*, *311*, 136990. https://doi.org/10.1016/j.chemosphere.2022.136990

X-ray Powder Diffraction (XRD). (n.d.). Techniques. Available at: https://serc.carleton.edu/research_education/geochemsheets/techniques/XRD.html (accessed: 23.03)

Yost, L. J., Shock, S. S., Holm, S. E., Lowney, Y. W., & Noggle, J. J. (2010). Lack of Complete Exposure Pathways for Metals in Natural and FGD Gypsum. *Human and Ecological Risk*

Assessment: An International Journal, *16*(2), 317–339.
https://doi.org/10.1080/10807031003670352

Norges miljø- og biovitenskapelige universitet
Noregs miljø- og biovitskapelege universitet
Norwegian University of Life Sciences

Postboks 5003
NO-1432 Ås
Norway